Binuclear Homoleptic Iron Carbonyls: Incorporation of Formal Iron−Iron Single, Double, Triple, and Quadruple Bonds, $Fe_2(CO)_x$ ($x = 9, 8, 7, 6$)

Yaoming Xie, Henry F. Schaefer III,* and R. Bruce King

Contribution from the Center for Computational Quantum Chemistry, Department of Chemistry, University of Georgia, Athens, Georgia 30602

Received April 3, 2000. Revised Manuscript Received May 26, 2000

Abstract: The homoleptic binuclear compound $Fe_2(CO)_9$ is well characterized experimentally, although there has been some discussion as to the nature of the iron−iron bond, which is at most a single bond. In this research, we consider homoleptic iron carbonyls that satisfy the 18-electron rule but may have formal double $Fe_2(CO)_8$ (seven distinct structures), triple $Fe_2(CO)_7$ (three distinct structures), and even quadruple $Fe_2(CO)_6$ (seven distinct structures) iron−iron bonds. These novel structures are characterized in terms of their equilibrium geometries, thermochemistry, and vibrational frequencies. The range of predicted iron−iron distances is remarkable, from 2.52 Å for the known $Fe_2(CO)_9$ to 2.00 Å for the unbridged quadruple bond species $Fe_2(CO)_6$. The lowest energy structure of $Fe_2(CO)_7$ is a distorted unbridged C_s symmetry structure with iron−iron separation 2.23 Å. This is followed energetically by the tribridged structure with bond distance 2.21 Å, and finally by the monobridged structure with iron−iron distance 2.13 Å. The latter structure is consistent with an Fe≡Fe triple bond, but is not a genuine minimum. For $Fe_2(CO)_6$ the lowest energy structure is the distorted dibridged structure with perhaps a weak Fe═Fe double bond. However, the unbridged $Fe_2(CO)_6$ structure with an iron−iron bond distance of 2.00 Å (suggesting a quadruple bond) is also a genuine minimum. The unsaturated structures $Fe_2(CO)_8$ and $Fe_2(CO)_7$, are thermodynamically resistant to CO removal. The iron−iron linkages are also analyzed in terms of contributions from the different vibrational potential energy distributions. A clear Badger's Rule correlation between Fe−Fe vibrational frequency and bond distance is established. Prospects for the synthesis of these and related diiron compounds are discussed in some detail. The most promising routes to preparation of these fascinating species would appear to be matrix isolation or iron vapor synthesis.

Introduction

Homoleptic transition metal carbonyls are fundamental constituents of modern organometallic chemistry.[1] The mononuclear closed-shell first row transition metal structures $Cr(CO)_6$, $Fe(CO)_5$, and $Ni(CO)_4$ are well known, as are the binuclear compounds $Fe_2(CO)_9$ and $Co_2(CO)_8$. The only stable, higher nuclearity, first row transition metal carbonyls are $Fe_3(CO)_{12}$, $Co_4(CO)_{12}$, and $Co_6(CO)_{16}$. Our interest in these compounds is 2-fold. First, why is it that compounds such as $Os_7(CO)_{21}$ exist, whereas the valence isoelectronic $Fe_7(CO)_{21}$ has never been made? The simple answer, of course, is that Os−Os bonds are stronger than Fe−Fe bonds, but we seek a deeper understanding. Our second interest is whether it might be possible to synthesize homoleptic transition metal carbonyls with *multiple* metal−metal bonds.[2]

In our earlier paper[3] on these subjects, we considered several possible nickel compounds, including the single-bonded $(CO)_3Ni(\mu\text{-}CO)Ni(CO)_3$, the Ni═Ni species $(CO)_2Ni(\mu\text{-}CO)_2Ni(CO)_2$, and the Ni≡Ni species $(CO)Ni(\mu\text{-}CO)_3Ni(CO)$. In the present research, the same general ideas are pursued in search of binuclear iron carbonyls with iron−iron multiple bonds. As we will see, the possibilities for the binuclear iron compounds are far more varied than those for the previously studied nickel systems. Experimentally, no nickel−nickel multiple bonds have been unambiguously characterized, and relatively few examples of iron−iron multiple bonding exist.[2]

Are there any precedents from experiment that might guide us in the present theoretical studies? Yes: $Fe_2(CO)_8$ was prepared as a transient species by Poliakoff and Turner[4] in 1971 and further characterized by Fletcher, Poliakoff, and Turner[5] in 1986, and by Fedrigo, Haslett, and Moskovits[6] in 1996. In fact, Fletcher, Poliakoff, and Turner[5] identified two different $Fe_2(CO)_8$ structures, the primary product apparently being the dibridged structure

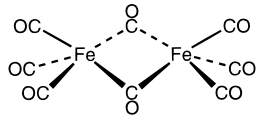

1

The second structure observed by Fletcher, Poliakoff, and Turner[5] was deduced to be an unbridged structure, and its infrared spectrum is consistent with the D_{2h} geometry predicted earlier from theory by Hoffmann.[7]

* To whom correspondence should be addressed.

(1) Cotton, F. A.; Wilkinson, G.; Murillo, C. A.; Bochmann, M. *Advanced Inorganic Chemistry*, 6th ed.; John Wiley: New York, 1999.

(2) Cotton, F. A.; Walton, R. A. *Multiple Bonds Between Metal Atoms*; Clarendon Press: Oxford, 1993.

(3) Ignatyev, I. S.; Schaefer, H. F.; King, R. B.; Brown, S. T. *J. Am. Chem. Soc.* **2000**, *122*, 1989.

(4) Poliakoff, M.; Turner, J. J. *J. Chem. Soc. A* **1971**, 2403.

(5) Fletcher, S. C.; Poliakoff, M.; Turner, J. J. *Inorg. Chem.* **1986**, *25*, 3597.

(6) Fedrigo, S.; Haslett, T. L.; Moskovits, M. *J. Am. Chem. Soc.* **1996**, *118*, 5083.

10.1021/ja001162y CCC: $19.00
Published on Web 08/25/2000

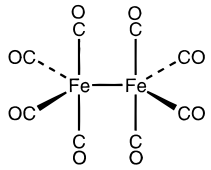

2

In his 1982 Nobel Lecture, Hoffmann sketches **2** with an Fe═Fe double bond.

The valence isoelectronic transient $Os_2(CO)_8$ was reported by three different research teams in 1990. Norton and co-workers[8] concluded that $Os_2(CO)_8$ has a structure with only terminal carbonyls, and they favor a D_{2h} structure analogous to **2** above with a closed-shell singlet electronic ground state. Bogdan and Weitz[9] drew no conclusions concerning the structure of $Os_2(CO)_8$. Grevels and co-workers[10] note that a D_{2h} structure is "logical on the basis of the isolobal analogy between a d^8 ML_4 dimer and ethylene", and they depict $Os_2(CO)_8$ with an Os═Os double bond in their Scheme 1 (p 1995). Several subsequent experimental papers,[11−13] relating to the $Os_2(CO)_8$ transient have appeared since 1990. In their 1997 paper, Ramage, Wiser, and Norton[12] characterize $Os_2(CO)_8$ as an Os═Os doubly bonded species in their eqs 3, 4, and 5.

There are two computational studies of the $Fe_2(CO)_8$ transient prepared by Poliakoff and Turner.[4,5] The first is the 1996 density functional work of Jacobsen and Ziegler.[14] The latter found the lowest energy structure to have two bridging CO ligands. The unbridged $Fe_2(CO)_8$, with a formal Fe═Fe double bond, is stabilized by a trans bent distortion and is predicted to lie 7 kcal/mol above the doubly bridged structure, consistent with the experiment of Poliakoff and Turner.[4,5] The second theoretical paper on $Fe_2(CO)_8$ is the recent density functional theory (DFT) study of Barckholtz and Bursten,[15] who reproduced the lowest energy structure of Jacobsen and Ziegler.[14] They also supported the experimental $Fe_2(CO)_9$ dissociation energies for Fe−Fe rupture (DFT 29.5 kcal/mol; experimental estimate[16] 29 kcal/mol) and for removal of one of the bridging carbonyls (DFT 32.3 kcal/mol; experiment[16] 28 kcal/mol).

The most recent experimental paper related to the present research is the mass spectrometric study of Markin and Sugawara.[17] The authors determined the following radical cation dissociation energies:

$$Fe_2(CO)_9^+ \rightarrow Fe_2(CO)_8^+ + CO \qquad \Delta E = 24.9 \pm 2.5 \text{ kcal/mol} \quad (1)$$

$$Fe_2(CO)_8^+ \rightarrow Fe_2(CO)_7^+ + CO \qquad \Delta E = 7.6 \pm 1.8 \text{ kcal/mol} \quad (2)$$

$$Fe_2(CO)_7^+ \rightarrow Fe_2(CO)_6^+ + CO \qquad \Delta E = 18.9 \pm 2.5 \text{ kcal/mol} \quad (3)$$

$$Fe_2(CO)_6^+ \rightarrow Fe_2(CO)_5^+ + CO \qquad \Delta E = 25.4 \pm 1.8 \text{ kcal/mol} \quad (4)$$

Thus, it is seen that the radical cations of the neutral structures investigated herein have been observed in the gas phase. We expect that the radical cation structures may be even more complicated than the closed-shell neutral geometries predicted here. The above experimental reaction energies indicate that $Fe_2(CO)_9^+$ and $Fe_2(CO)_6^+$ are relatively stable, while $Fe_2(CO)_8^+$ loses a carbonyl ligand very easily.

Theoretical Methods

Our basis set for C and O begins with Dunning's standard double-ζ contraction[18] of Huzinaga's primitive sets[19] and is designated (9s5p/4s2p). The double-ζ plus polarization (DZP) basis set used here adds one set of pure spherical harmonic d functions with orbital exponents $\alpha_d(C) = 0.75$ and $\alpha_d(O) = 0.85$ to the DZ basis set. For Fe, in our loosely contracted DZP basis set, the Wachters' primitive set,[20] is used, but augmented by two sets of p functions and one set of d functions, contracted following Hood et al.,[21] and designated (14s11p6d/10s8p3d). For $Fe_2(CO)_9$, there are 368 contracted Gaussian functions in the present DZP basis set.

Electron correlation effects were included employing DFT methods, which have been widely proclaimed as a practical and effective computational tool, especially for organometallic compounds. Among density functional procedures, the most reliable approximation is often thought to be the hybrid Hartree−Fock (HF)/DFT method using the combination of the three-parameter Becke exchange functional with the Lee−Yang−Parr nonlocal correlation functional known as B3LYP.[22,23] However, another DFT method, which combines Becke's 1988 exchange functional with Perdew's 1986 nonlocal correlation functional method (BP86), was also used in the present paper for comparison.[24,25]

We fully optimized the geometries of all structures with the DZP B3LYP and DZP BP86 methods. At the same levels we also report the vibrational frequencies by evaluating analytically the second derivatives of the energy with respect to the nuclear coordinates. The corresponding infrared intensities are evaluated analytically as well. All of the computations were carried out with the Gaussian 94 program,[26] in which the fine grid (75 302) is the default for evaluating integrals numerically, and the tight (10^{-8} hartree) designation is the default for the self-consistent field (SCF) convergence. Cases for which larger integration grids were used will be discussed later.

The results from these computations are depicted in Figures 2−12 with all bond distances given in Å.

Results and Discussion

A. Molecular Structures. I. $Fe_2(CO)_9$. We previously reported and discussed the D_{3h} structure of $Fe_2(CO)_9$ at the DZP B3LYP and DZP BP86 levels of theory.[27] Because this is the only experimentally known structure[28] in the family investigated here, we show the structure of $Fe_2(CO)_9$ in Figure 1.

(7) Hoffmann, R. *Angew. Chem., Int. Ed. Engl.* **1982**, *21*, 711.
(8) Haynes, A.; Poliakoff, M.; Turner, J. J.; Bender, B. R.; Norton, J. R. *J. Organomet. Chem.* **1990**, *383*, 497.
(9) Bogdan, P. L.; Weitz, E. *J. Am. Chem. Soc.* **1990**, *112*, 639.
(10) Grevels, F.-W.; Klotzbücher, W. E.; Seils, F.; Schaffner, K.; Takats, J. *J. Am. Chem. Soc.* **1990**, *112*, 1995.
(11) Burke, M. R.; Seils, F.; Takats, J. *Organometallics* **1994**, *13*, 1445.
(12) Ramage, D. L.; Wiser, D. C.; Norton, J. R. *J. Am. Chem. Soc.* **1997**, *119*, 5618.
(13) Bender, B. R.; Ramage, D. L.; Norton, J. R.; Wiser, D. C.; Rappe, A. K. *J. Am. Chem. Soc.* **1997**, *119*, 5628.
(14) Jacobsen, H.; Ziegler, T. *J. Am. Chem. Soc.* **1996**, *118*, 4631.
(15) Barckholtz, T. A.; Bursten, B. E. *J. Organomet. Chem.* **2000**, *596*, 212.
(16) Baev, A. K. *Russ. J. Phys. Chem.* **1980**, *54*, 1.
(17) Markin, E. M.; Sugawara, K. *J. Phys. Chem. A* **2000**, *104*, 1416.
(18) Dunning, T. H. *J. Chem. Phys.* **1970**, *53*, 2823.
(19) Huzinaga, S. *J. Chem. Phys.* **1965**, *42*, 1293.
(20) Wachters, A. J. H. *J. Chem. Phys.* **1970**, *52*, 1033.
(21) Hood, D. M.; Pitzer, R. M.; Schaefer, H. F. *J. Chem. Phys.* **1979**, *71*, 705.
(22) Becke, A. D. *J. Chem. Phys.* **1993**, *98*, 5648.
(23) Lee, C.; Yang, W.; Parr, R. G. *Phys. Rev. B* **1988**, *37*, 785.
(24) Becke, A. D. *Phys. Rev. A* **1988**, *38*, 3098.
(25) Perdew, J. P. *Phys. Rev. B* **1986**, *33*, 8822.
(26) Frisch, M. J.; Trucks, G. W.; Schlegel, H. B.; Gill, P. M. W.; Johnson, B. G.; Robb, M. A.; Cheeseman, J. R.; Keith, T.; Petersson, G. A.; Montgomery, J. A.; Raghavachari, K.; Al-Laham, M. A.; Zakrzewski, V. G.; Ortiz, J. V.; Foresman, J. B.; Peng, C. Y.; Ayala, P. Y.; Chen, W.; Wong, M. W.; Andres, J. L.; Replogle, E. S.; Gomperts, R.; Martin, R. L.; Fox, D. J.; Binkley, J. S.; Defrees, D. J.; Baker, J.; Stewart, J. J. P.; Head-Gordon, M.; Gonzalez, C.; Pople, J. A. *GAUSSIAN 94*, Revision B.3; Gaussian, Inc.: Pittsburgh, PA, 1995.
(27) Jang, J. H.; Lee, J. G.; Lee, H.; Xie, Y.; Schaefer, H. F. *J. Phys. Chem. A* **1998**, *102*, 5298.
(28) Cotton, F. A.; Troup, J. M. *J. Chem. Soc., Dalton Trans.* **1974**, 800.

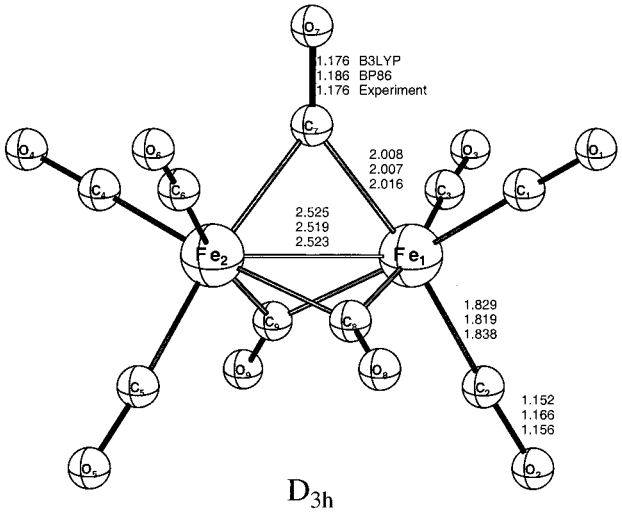

Figure 1. The tribridged structure of $Fe_2(CO)_9$, tri-μ-carbonylhexacarbonyldiiron. The experimental structure is from ref 28.

II. $Fe_2(CO)_8$. Seven $Fe_2(CO)_8$ structures were optimized in this research and they are reported in Figures 2, 3, and 4. Figure 2a shows the C_{2v} dibridged structure reported as most stable in the experiments of Fletcher, Poliakoff, and Turner.[4,5] This structure is a genuine minimum with both B3LYP and BP86 methods. The iron−iron bond distance is predicted to be 2.443 Å (DZP B3LYP), or 0.082 Å shorter than that for the stable compound $Fe_2(CO)_9$. With the DZP BP86 method, the Fe−Fe bond distance shrinkage from $Fe_2(CO)_9$ to the dibridged structure of $Fe_2(CO)_8$ is 0.072 Å. To satisfy the 18-electron rule, the dibridged structure seen in Figure 2a must incorporate an Fe═Fe double bond, and we do see a significant reduction in this bond distance compared to the classical $Fe_2(CO)_9$. Note that the present predicted iron−iron distances (2.443 and 2.447 Å) are significantly shorter than the 2.506 Å reported in the earlier DFT study of Jacobsen and Ziegler.[14] Figure 2b shows another dibridged $Fe_2(CO)_8$ structure with C_{2h} symmetry. It lies 3.2 (B3LYP) or 2.2 (BP86) kcal/mol higher in energy than the C_{2v} structure, and it has two small imaginary vibrational frequencies.

The unbridged D_{2h} structure of $Fe_2(CO)_8$ predicted by Hoffmann[7] in 1982 and supported by the 1987 experiments of Fletcher, Poliakoff, and Turner[5] is shown in Figure 3a. Our predicted iron−iron distances (2.542 Å B3LYP, 2.551 Å BP86) are slightly longer (by 0.017 and 0.032 Å, respectively) than the comparable distance in the stable compound $Fe_2(CO)_9$. This confirms the expectation of Fedrigo, Haslett, and Moskovits[6] that the iron−iron distance in the unbridged $Fe_2(CO)_8$ should "be comparable to that found in the nonacarbonyl." Thus there is no evidence for an Fe═Fe double bond from the structural perspective. Note that our predicted iron−iron distances are much shorter than the 2.671 Å reported in the earlier DFT study of Jacobsen and Ziegler.[14] This structure has two small imaginary vibrational frequencies.

Following Jacobsen and Ziegler,[14] we also located a C_{2h} symmetry distorted unbridged structure of $Fe_2(CO)_8$, and this is seen in Figure 3b, with one small imaginary vibrational frequency. Although the distortion from D_{2h} (Figure 3a) to C_{2h} lowers the energy, the Fe−Fe distance for the latter structure increases to 2.607 Å (B3LYP) or 2.585 Å (BP86). Presumably, this central bond distance lengthening allows the two centrally located carbonyl groups to move in the direction of the dibridged structure (Figure 2a). In any case, Figure 3b shows no structural sign of an Fe═Fe double bond. Figures 3c and 3d show two other unbridged $Fe_2(CO)_8$ structures, one of which has C_{2h} symmetry and the other D_{2d}. Both are high lying energetically, and have imaginary vibrational frequencies.

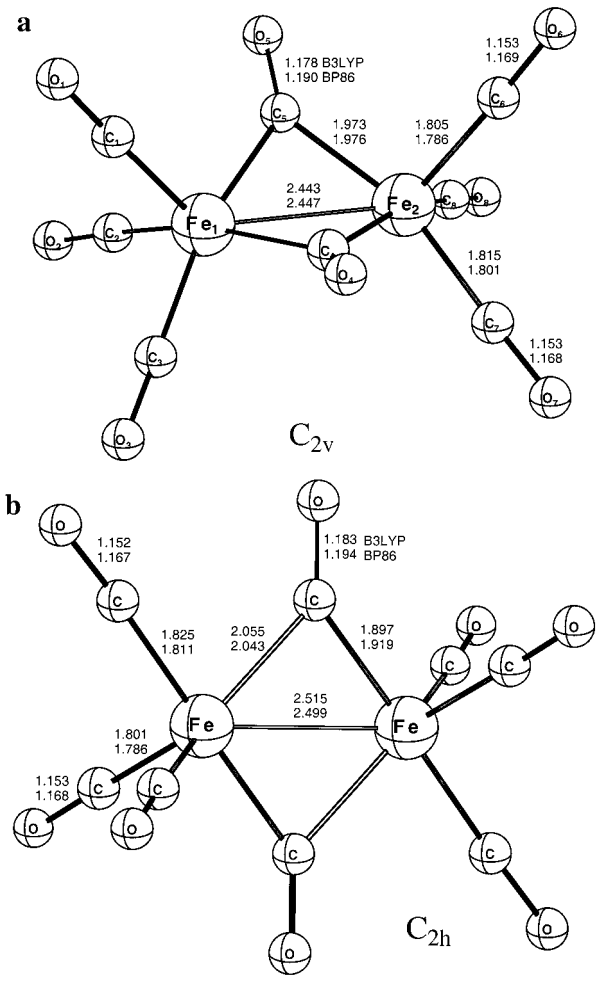

Figure 2. (a) The dibridged structure of $Fe_2(CO)_8$, di-μ-carbonylhexacarbonyldiiron. This is the lowest energy structure predicted for $Fe_2(CO)_8$. (b) The C_{2h} distorted dibridged structure of $Fe_2(CO)_8$. This structure lies energetically higher than the dibridged C_{2v} structure by 3.2 B3LYP or 2.2 kcal/mol (BP86).

Our final structure for $Fe_2(CO)_8$ is the tetrabridged geometry seen in Figure 4. This structure was not considered by the earlier experimental[4,5] or theoretical[14] studies. With respect to its iron−iron distance, the tetrabridged structure is the most interesting of the $Fe_2(CO)_8$ geometries considered. The iron−iron distance is 2.318 Å (B3LYP) or 2.331 Å (BP86). These distances are shorter than those for the stable $Fe_2(CO)_9$ molecules by 0.207 Å (B3LYP) and 0.188 Å (BP86), respectively. Thus, from a structural perspective, the tetrabridged $Fe_2(CO)_8$ could surely be inferred to have an Fe═Fe double bond. However, we will see that this structure is quite high-lying energetically.

We also tried to optimize an asymmetric unbridged structure for $Fe_2(CO)_8$, such as $(CO)_5Fe-Fe(CO)_3$, but no such stationary point was located and trial geometries in this region eventually collapse to the structures discussed above.

III. $Fe_2(CO)_7$. To satisfy the 18-electron rule, conventional $Fe_2(CO)_7$ structures should incorporate a formal Fe≡Fe triple bond. Our monobridged structure, seen in Figure 5, does indeed display a remarkably short iron−iron distance. With the B3LYP method r_e(Fe−Fe) = 2.132 Å and with the BP86 method r_e-(Fe−Fe) = 2.137 Å. These distances are 0.393 and 0.382 Å, respectively, shorter than those at the same levels of theory for the stable $Fe_2(CO)_9$ structure. Thus, from a structural viewpoint,

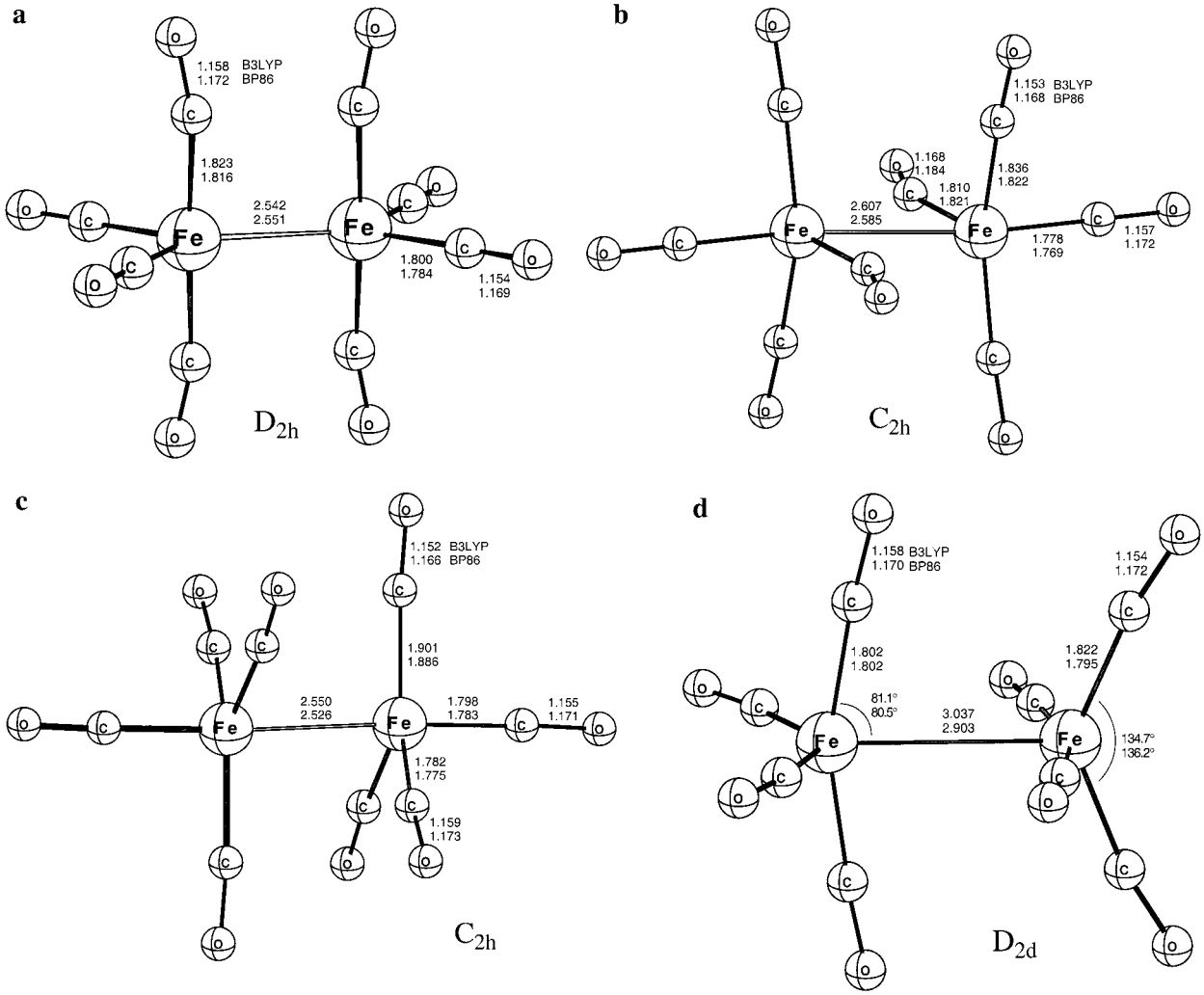

Figure 3. (a) The unbridged structure of $Fe_2(CO)_8$, octacarbonyldiiron. (b) The C_{2h} distorted unbridged structure of $Fe_2(CO)_8$. This structure lies energetically lower than the unbridged D_{2h} structure by 8.5 (B3LYP) or 9.3 kcal/mol (BP86). (c) The C_{2h} unbridged structure of $Fe_2(CO)_8$. (d) The D_{2d} unbridged structure of $Fe_2(CO)_8$.

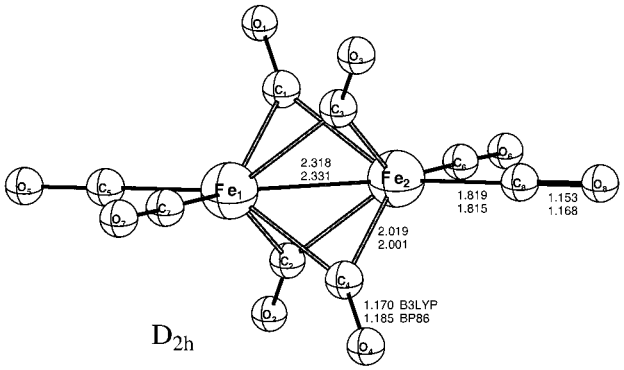

Figure 4. The tetrabridged structure of $Fe_2(CO)_8$, tetra-μ-carbonyltetracarbonyldiiron.

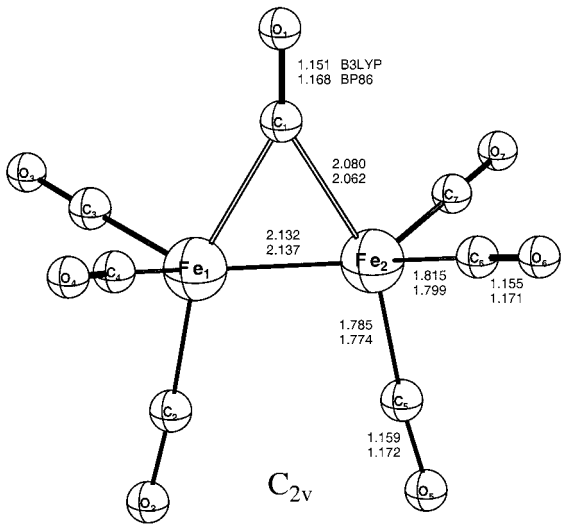

Figure 5. The monobridged structure of $Fe_2(CO)_7$, μ-carbonylhexacarbonyldiiron.

one could reasonably conclude that an Fe≡Fe triple bond is predicted from theory. However, we will see that this structure is not a genuine minimum.

Also investigated in this research was the tribridged $Fe_2(CO)_7$ structure seen in Figure 6. The iron−iron distance here is somewhat longer than predicted for the monobridged structure just discussed. Specifically, the iron−iron distance for the tribridged structure is 0.080 Å (B3LYP) or 0.071 Å (BP86) longer than that for the monobridged $Fe_2(CO)_7$ structure. If one takes the view that the transition from one bond type (e.g., single bond) to the adjacent stronger bond type (double bond in this case) should be accompanied by an internuclear separation decreasing by 0.2 Å, then the tribridged $Fe_2(CO)_7$ might be argued to have bond order 5/2.

The structure of $Fe_2(CO)_7$ with the lowest energy is seen in Figure 7 and has two highly unsymmetrical bridging carbonyls.

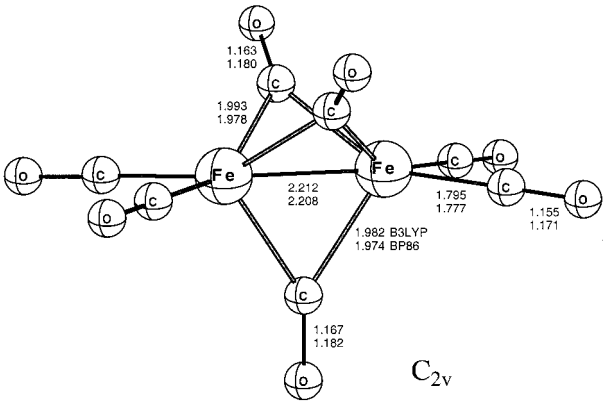

Figure 6. The tribridged structure of $Fe_2(CO)_7$, tri-μ-carbonyltetracarbonyldiiron.

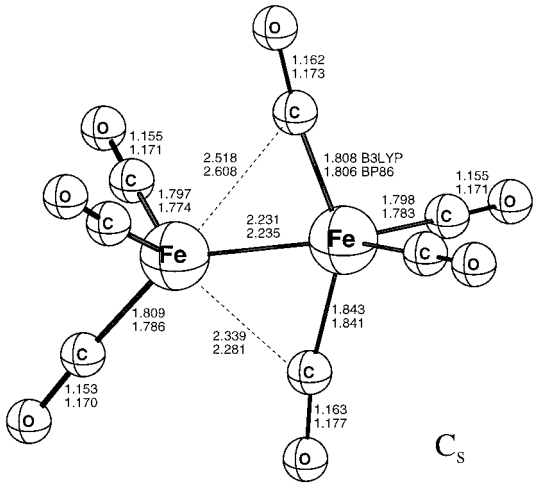

Figure 7. The C_s distorted structure of $Fe_2(CO)_7$ with two highly unsymmetrical bridging carbonyls. This is the lowest energy structure predicted for $Fe_2(CO)_7$.

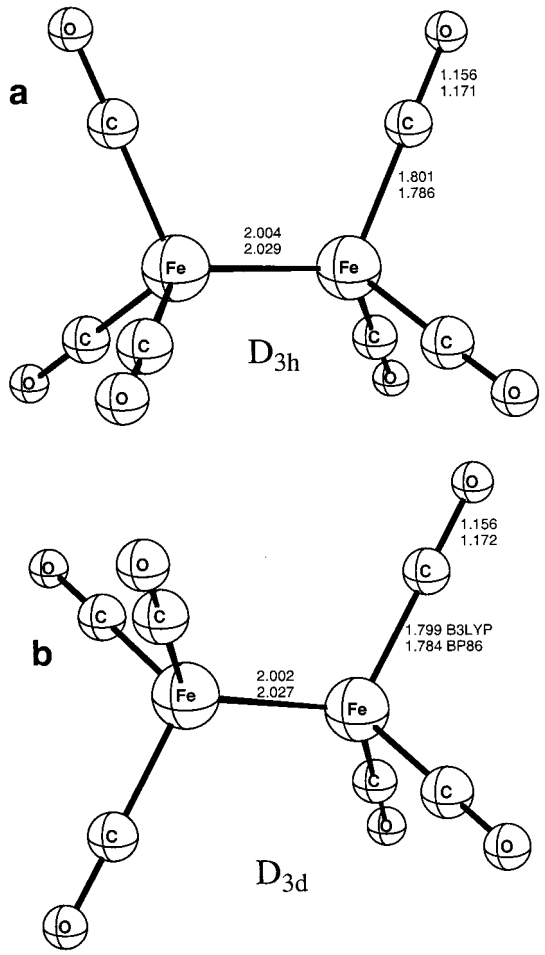

Figure 8. The unbridged structure of $Fe_2(CO)_6$, hexacarbonyldiiron.

It has C_s symmetry, and it is a genuine minimum. The central bond distance predicted for this interesting structure is 2.231 Å (B3LYP), which again would relate to a bond order something like 5/2.

IV. $Fe_2(CO)_6$. For the reader who may think that iron dimers with this few carbonyl ligands are ultraexotic, we emphasize that the radical cation of $Fe_2(CO)_6$ has been observed in the gas phase and characterized thermochemically.[17] In addition, we would not be surprised to see neutral $Fe_2(CO)_6$ observed by matrix isolation techniques soon.[29]

Our most favorable unbridged $Fe_2(CO)_6$ structures are seen in Figure 8. The eclipsed (D_{3h}) and staggered (D_{3d}) structures have almost the same bond distances (within 0.002 Å), and they are near-degenerate in energy with D_{3h} structure lower by only 1.15 (B3LYP) or 0.49 (BP86) kcal/mol. The D_{3h} structure is a genuine minimum, and the D_{3d} one has one or two tiny imaginary vibrational frequencies. Therein is the shortest Fe−Fe distance predicted in this research, namely 2.00 Å (B3LYP) or 2.03 Å (BP86). This distance is shorter than that in the stable $Fe_2(CO)_9$ by 0.52 Å (B3LYP) or 0.49 Å (BP86). By the criterion discussed in the previous subsection, these unbridged $Fe_2(CO)_6$ structures would have a bond order between 3 and 4.

Our first dibridged $Fe_2(CO)_6$ structure is reported in Figure 9a, and it has two substantial imaginary vibrational frequencies. Although electron counting gives the dibridged structure a quadruple bond, the predicted bond distances would seem to exclude this possibility. By the structural criteria developed here (0.2 Å decrease in the metal−metal distance with an increase of one in bond order), the iron−iron distances of 2.416 Å (B3LYP) and 2.398 Å (BP86) suggest a weak double bond for the structure seen in Figure 9a.

Distortion of the above D_{2h} structure to C_{2h} symmetry results in an energy lowering and the distorted dibridged $Fe_2(CO)_6$ structure seen in Figure 9b. This C_{2h} structure is our lowest lying energetically for $Fe_2(CO)_6$. As was the case with our earlier Figure 3a/3b comparison, relaxation to lower symmetry lengthens the iron−iron separation, in this case to 2.435 Å (B3LYP) or 2.434 Å (BP86). As with Figure 9a, the best structural characterization of Figure 9b is as a weak double bond. Distortion of the D_{2h} structure (Figure 9a) to C_{2v} symmetry leads to a small energy lowering and the C_{2v} dibridged structure seen in Figure 9c.

An asymmetric unbridged $Fe_2(CO)_6$ structure, i.e., $(CO)_4Fe-Fe(CO)_2$, was optimized as a stationary point with C_{2v} symmetry, and is shown in Figure 10. Rotating around the Fe−Fe bond, we can have another C_{2v} structure with somewhat lower energy, shown in Figure 11. Following the normal mode of an imaginary vibrational frequency, we were able to optimize a C_s monobridged structure (Figure 12).

V. Structure and Bonding. With the extraordinary range of structures predicted here, it would not be surprising to find traditional models of bonding and electronic structure less than entirely satisfactory. One of the two referees noted that "it is not obvious how such bond orders are arising." Because it is commonly stated that the bonding in the stable $Fe(CO)_5$ molecule involves a d^8 iron atom, the referee continues that it

(29) See, for example, the zirconium and hafnium carbonyls recently observed by Zhou, M.; Andrews, L. *J. Am. Chem. Soc.* **2000**, *122*, 1531.

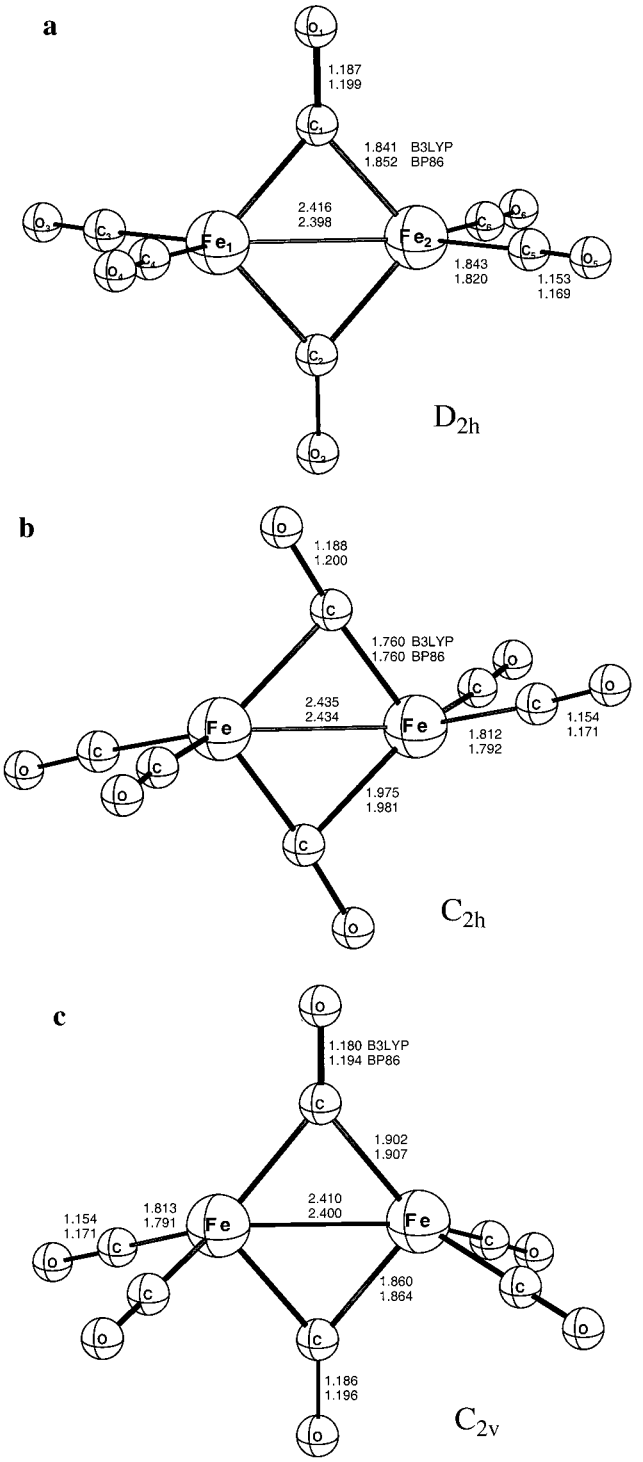

Figure 9. (a) The D_{2h} dibridged structure of $Fe_2(CO)_6$, di-μ-carbonyltetracarbonyldiiron. (b) The C_{2h} trans-dibridged structure of $Fe_2(CO)_6$. This is the lowest energy structure predicted for $Fe_2(CO)_6$. (c) The C_{2v} dibridged structure of $Fe_2(CO)_6$.

might not be unreasonable to assume that the iron atoms in these binary carbonyls might also reflect a d^8 iron atom configuration. If this were the case, with three doubly occupied and two singly occupied 3d components, then only iron−iron single and double bonds are readily constructed in a simple bonding picture. The referee suggested three possible simple pictures of higher iron−iron bond orders: (a) species with one-electron bonds; (b) iron configuration promotion to d^7s; and (c) Fe^+ or Fe^{2+} arrangements. However, (a) seems unlikely because our most stable structures are closed-shell singlets, (b) would seem to lead to

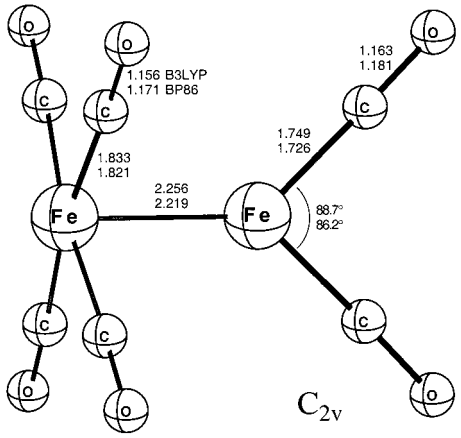

Figure 10. The unsymmetrical unbridged structure of $Fe_2(CO)_6$, hexacarbonyldiiron.

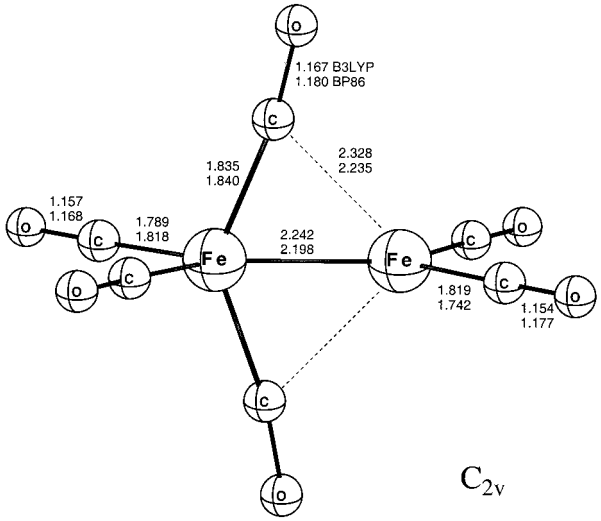

Figure 11. A structure of $Fe_2(CO)_6$ with two highly unsymmetrical bridging carbonyl groups.

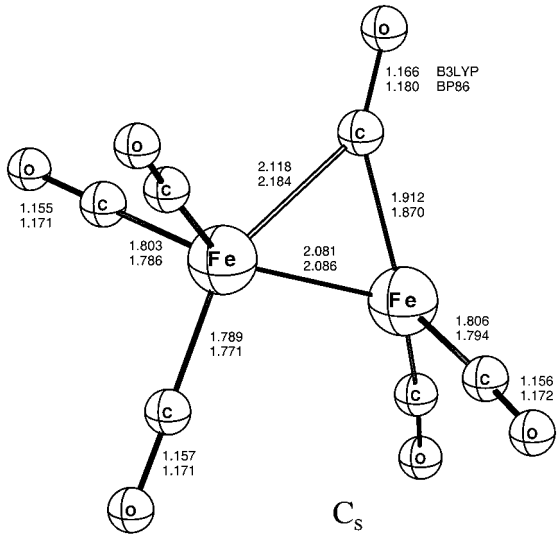

Figure 12. The monobridged structure of $Fe_2(CO)_6$, μ-carbonylpentacarbonyldiiron.

Fe−CO repulsion, and (c) would seem to lead to Fe−Fe electrostatic repulsion. Thus, one may need new insights from qualitative molecular orbital theory to explain the variety of structures predicted here.

Suggestions (b) and (c) above may be pursued in terms of theoretical iron atom populations. For our quadruple bond Fe_2-

Table 1. Dissociation Energies (in kcal/mol) for $Fe_2(CO)_n \rightarrow Fe_2 + n\ CO$

n	formal central bond	sym.	Fe−Fe bond length (Å)	no. of bridges	figure no. in text	imaginary freq. B3LYP	imaginary freq. BP86	B3LYP	per CO	BP86	per CO	expt.	per CO
6	Fe⁴Fe	D_{3d}	2.002	0	8a	18*i*	11*i*, 8*i*	173.0	28.8	250.9	41.8		
	Fe⁴Fe	D_{3h}	2.004	0	8b	none	none	174.1	29.0	251.3	41.9		
	Fe⁴Fe	D_{2h}	2.416	2	9a	414*i*, 202*i*, 65*i*	389*i*, 235*i*	171.6	28.6	255.2	42.5		
	Fe⁴Fe	C_{2h}	2.435	2	9b	none	33*i*	186.2	31.0	267.3	44.6		
	Fe⁴Fe	C_{2v}	2.410	2	9c	none	none	180.6	30.1	264.2	44.0		
	Fe⁴Fe	C_{2v}	2.256	0	10	54*i*	82*i*, 19*i*	159.2	26.5	235.4	39.2		
	Fe⁴Fe	C_{2v}	2.242	0	11	374*i*, 11*i*	63*i*, 16*i*	166.4	27.7	245.0	40.8		
	Fe⁴Fe	C_s	2.081	1	12	32*i*	31*i*	177.9	29.7	256.8	42.8		
7	Fe≡Fe	C_{2v}	2.132	1	5	490*i*, 72*i*, 70*i*, 64*i*	487*i*, 82*i*, 31*i*, 61*i*	200.2	28.6	283.9	40.6		
	Fe≡Fe	C_s	2.231	0	7	none	none	218.8	31.3	301.3	43.0		
	Fe≡Fe	C_{2v}	2.212	3	6	90*i*	67*i*	208.9	29.8	297.6	42.5		
8	Fe═Fe	D_{2h}	2.542	0	3a	39*i*, 30*i*, 15*i*	61*i*, 28*i*, 12*i*	233.8	29.2	325.3	40.7		
	Fe═Fe	C_{2h}	2.607	0	3b	95*i*	15*i*	242.2	30.3	334.6	41.8		
	Fe═Fe	C_{2v}	2.443	2	2a	none	none	244.2	30.5	338.8	42.4		
	Fe═Fe	D_{2h}	2.318	4	4	367*i*, 307*i*, 171*i*, 106*i*	316*i*, 146*i*, 102*i*, 44*i*	169.6	21.2	279.4	34.9		
	Fe═Fe	C_{2h}	2.550	0	3c	254*i*, 96*i*, 37*i*	198*i*, 87*i*, 39*i*	225.2	28.2	319.5	39.9		
	Fe═Fe	D_{2d}	3.037	0	3d	49*i*, 22*i*, 8*i*	10*i*	223.3	27.9	308.1	38.5		
	Fe═Fe	C_{2h}	2.515	2	2b	45*i*, 32*i*	43*i*, 28*i*	240.9	30.1	336.7	42.1		
9	Fe−Fe	D_{3h}	2.525	3	1	none	none	273.6	30.4	373.9	41.5	253 ± 9[a]	28 ± 1

[a] See text for the sources of this experimental result.

$(CO)_6$ structures, Figure 8a,b, the Fe B3LYP populations indicate $s^{0.60}d^{7.03}$ (D_{3d}) or $s^{0.58}d^{7.04}$ (D_{3h}), suggesting that option (b) above may be plausible. However, the overall charge on iron in the quadruple bond $Fe_2(CO)_6$ structure is −0.13, confirming that a simple explanation along the lines of idea (c) above is less than promising.

The assignment of bond orders for structures such as those studied here is an inherently risky business, particularly for systems incorporating bridging carbonyls.[30−32] Our use of the term "formal bond order" is meant to convey a cautious application of the 18-electron rule. Jemmis, Pinhas, and Hoffmann note in their 1980 paper,[32] "It may be indeed pleasing or even correct to assign a metal−metal bond order to a given compound. But we view this as a description of nature and not as its understanding."

Hoffmann made some interesting comments[33] in this regard on our unbridged D_{2h} structure, seen in Figure 3a. He notes that the axial carbonyls are bent away, while the C−Fe−Fe bonds are near 90°. In all of our structures, no other carbonyls except those with incipient bridging are bent in this manner. Clearly, the carbonyls repel each other, and Hoffmann observes that to get two CO's into a π-impacting configuration is costly energetically. As an experimental example of this sort of behavior Hoffmann notes Vahrenkamp's 1978 compound[34] with a V═V double bond. Thus Hoffmann concludes that our Figure 3a, while exhibiting a 2.54 Å iron−iron bond distance seemingly characteristic of a single bond, is in fact doubly bonded.

B. Thermochemistry. There are several possible ways to evaluate the thermochemistry of the $Fe_2(CO)_x$ species. One of these, dissociation to $Fe_2 + n$ CO, is displayed in Table 1. There is one experimental dissociation energy in Table 1, and we should explain its origin. The enthalpy of reaction of

$$Fe_2(CO)_9 \rightarrow 2Fe + 9CO \qquad \Delta H°(298) = +279.8 \pm 6.5\ \text{kcal/mol} \quad (5)$$

was calculated from the experimental heats of formation of $Fe_2(CO)_9$ (-319 ± 6 kcal), Fe (99.31 ± 0.06 kcal), and CO (26.42 ± 0.04 kcal) given by Markin and Sugawara.[17] To this we add the experimental dissociation energy of Fe_2

$$Fe + Fe \rightarrow Fe_2\ D_o = -26.5 \pm 2.1\ \text{kcal/mol} \quad (6)$$

from Loh, Lian, Hales, and Armentrout.[35] Adding eqs 5 and 6 gives us the desired dissociation

$$Fe_2(CO)_9 \rightarrow Fe_2 + 9CO \qquad \Delta H = 253.3 \pm 8.6\ \text{kcal/mol} \quad (7)$$

The DZP B3LYP dissociation energy (eq 7) is 273.6 kcal/mol, in reasonable agreement with experiment. However, the BP86 result, 373.9 kcal/mol, is much larger than experiment. The same pattern between B3LYP and BP86 is observed for the other dissociation energies in Table 1. Thus, we conclude that the B3LYP thermochemistry is superior for these systems.

Table 1 provides the relative energies for the different $Fe_2(CO)_x$ structures. Thus, we see that among possible $Fe_2(CO)_8$ structures, the C_{2v} dibridged geometry seen in Figure 2a lies lowest in energy. The unbridged D_{2h} structure (Figure 3a) lies 10.4 kcal/mol higher than the dibridged $Fe_2(CO)_8$ structure. However, the distorted unbridged structure (Figure 3b), of C_{2h} symmetry, lies only 2.0 kcal/mol (B3LYP) above the dibridged structure. With the BP86 method, the distorted unbridged structure lies 4.2 kcal/mol above the dibridged structure (Figure 2). Either of our B3LYP or BP86 energetics show the dibridged/distorted unbridged energy difference to be less than the 7 kcal/mol predicted by Jacobsen and Ziegler.[13]

Turning to the three $Fe_2(CO)_7$ structures, one sees in Table 1 that the tribridged structure (Figure 6) lies lower by 8.7 kcal/mol (B3LYP) than the monobridged structure (Figure 5). In this case the lower energy tribridged structure ($r_e = 2.212$ Å) is predicted to have a longer bond distance than the monobridged structure ($r_e = 2.132$ Å). With the BP86 method, the tribridged structure again lies lower, but by a larger amount, 13.7 kcal/mol. The best $Fe_2(CO)_7$ structure energetically is that seen in Figure 7, the distorted unbridged structure of C_s symmetry. With the B3LYP method, this unbridged structure lies 9.9 kcal/mol

(30) Thorn, D. L.; Hoffmann, R. *Inorg. Chem.* **1978**, *17*, 126.
(31) Dedieu, A.; Albright, T. A.; Hoffmann, R. *J. Am. Chem. Soc.* **1979**, *101*, 3141.
(32) Jemmis, E. D.; Pinhas, A. R.; Hoffmann, R. *J. Am. Chem. Soc.* **1980**, *102*, 2576.
(33) Hoffmann, R. Personal communication, June 2000.
(34) Vahrenkamp, H. *Chem. Ber.* **1978**, *111*, 3472.
(35) Loh, S. K.; Lian, L.; Hales, D. A.; Armentrout, P. B. *J. Phys. Chem.* **1988**, *92*, 4009.

Table 2. Dissociation Energies (kcal/mol) for the Successive Removal of Carbonyls from $Fe_2(CO)_9$; All Results Reported Here Refer to the Lowest Energy Structures of $Fe_2(CO)_n$

	B3LYP	BP86	experiment[a]
$Fe_2(CO)_9 \rightarrow Fe_2(CO)_8 + CO$	29.4	35.1	28
$Fe_2(CO)_8 \rightarrow Fe_2(CO)_7 + CO$	25.4	37.6	
$Fe_2(CO)_7 \rightarrow Fe_2(CO)_6 + CO$	32.6	33.9	

[a] From ref 16.

below the tribridged $Fe_2(CO)_7$. This energy separation is smaller, 3.7 kcal/mol, with the BP86 method.

For the $Fe_2(CO)_6$ system, from the DZP B3LYP method, the extremely short iron−iron bond (r_e = 2.00 Å) goes with the unbridged structures (Figure 8a,b), which lie lower in energy by 1.4−2.5 kcal/mol than the dibridged structure (Figure 9a). Recall that these unbridged structures could plausibly be classified as incorporating an Fe$\overset{4}{—}$Fe quadruple bond. The dibridged $Fe_2(CO)_6$ seen in Figure 9a has a much longer bond distance. It is disconcerting that the BP86 method gives the opposite ordering, with the dibridged structure predicted to lie lower by 3.9−4.3 kcal/mol. Thus, we cannot definitively predict whether the unbridged or dibridged structure lies lower. We do want to emphasize that our two DFT methods are in close agreement in their predictions of the equilibrium geometries of the $Fe_2(CO)_6$ structures. The uneven ordering of the unbridged and dibridged D_{2h} structures became less important with our

Table 3

A. Harmonic Vibrational Frequencies (in cm^{-1}) and Infrared Intensities (in Parentheses, in km/mol) for Di-μ-carbonylhexacarbonyldiiron, Dibridged $Fe_2(CO)_8$; This C_{2v} Symmetry Structure Is the Lowest in Energy of All the $Fe_2(CO)_8$ Structures

	B3LYP DZP	BP86 DZP	expt.		B3LYP DZP	BP86 DZP	expt.
a_2	14 (0)	11 (0)		b_1	427 (8)	431 (1)	
b_1	16 (0)	6 (0)		b_1	457 (18)	466 (11)	
a_1	33 (0)	33 (0)		b_2	458 (5)	485 (2)	
b_2	75 (1)	76 (0)		a_1	468 (6)	482 (9)	
a_2	75 (0)	75 (0)		a_2	469 (0)	481 (0)	
a_1	81 (0)	80 (0)		a_1	470 (25)	489 (4)	
b_1	83 (0)	82 (0)		b_1	492 (1)	472 (2)	
a_1	96 (0)	92 (0)		b_2	515 (0)	537 (2)	
b_1	103 (1)	98 (0)		a_2	535 (0)	530 (0)	
a_2	103 (0)	110 (0)		a_1	558 (0)	551 (2)	
b_2	107 (0)	104 (0)		b_2	582 (103)	572 (59)	
b_2	109 (6)	112 (2)		b_1	582 (141)	584 (124)	
a_1	113 (0)	109 (0)		a_1	609 (93)	599 (89)	
a_2	209 (0)	220 (0)		a_2	612 (0)	606 (0)	
b_2	221 (4)	228 (0)		a_1	619 (31)	619 (19)	
a_1	231 (0)	227 (0)		b_2	625 (309)	623 (321)	
a_2	319 (0)	329 (0)		b_1	1885 (1079)	1841 (730)	1814[a]
b_2	362 (18)	407 (0)		a_1	1938 (185)	1870 (148)	1857[a]
b_1	368 (0)	365 (0)		b_2	2083 (328)	1993 (17)	1867 vw[b]
a_1	375 (0)	375 (0)		a_2	2086 (0)	2000 (0)	
b_1	393 (0)	389 (0)		b_1	2092 (1570)	2006 (1348)	2022[a]
a_2	395 (0)	402 (0)		a_1	2094 (1641)	2001 (1442)	2032[a]
a_1	421 (4)	418 (3)		b_2	2106 (2390)	2030 (1779)	2055[a]
b_2	425 (24)	428 (14)		a_1	2159 (4)	2068 (13)	

B. Harmonic Vibrational Frequencies (in cm^{-1}) and Infrared Intensities (in Parentheses, in km/mol) for Octacarbonyldiiron, Dibridged $Fe_2(CO)_8$ of Point Group Symmetry C_{2h}

	B3LYP DZP	BP86 DZP		B3LYP DZP	BP86 DZP
b_g	45*i*	43*i*	b_u	437 (8)	448 (1)
a_u	32*i*	28*i*	b_g	469 (0)	455 (0)
a_u	17 (0)	17 (0)	a_g	471 (0)	488 (0)
b_u	72 (1)	73 (0)	b_u	474 (31)	492 (13)
a_g	78 (0)	76 (0)	a_g	478 (0)	491 (0)
b_g	88 (0)	84 (0)	a_u	479 (20)	495 (8)
b_u	90 (1)	88 (0)	b_g	481 (0)	480 (0)
a_u	91 (0)	88 (0)	a_g	554 (0)	552 (0)
a_g	95 (0)	91 (0)	a_u	557 (9)	545 (4)
a_u	107 (1)	101 (1)	b_g	566 (0)	576 (0)
b_u	115 (0)	111 (0)	b_u	566 (121)	570 (123)
b_g	118 (0)	111 (0)	b_u	593 (118)	580 (52)
a_g	124 (0)	122 (0)	a_g	602 (0)	591 (0)
a_g	211 (0)	212 (0)	a_u	632 (123)	619 (107)
b_u	235 (2)	241 (1)	b_u	650 (276)	643 (317)
a_g	243 (0)	245 (0)	a_g	653 (0)	642 (0)
b_g	353 (0)	350 (0)	b_u	1867 (1033)	1825 (754)
b_u	368 (18)	400 (0)	a_g	1900 (0)	1845 (0)
a_u	370 (2)	387 (1)	b_g	2087 (0)	1994 (0)
a_g	386 (0)	390 (0)	a_u	2095 (1718)	2004 (1526)
a_u	390 (1)	367 (1)	a_g	2097 (0)	2008 (0)
b_u	409 (36)	417 (11)	b_u	2100 (1477)	2011 (1294)
b_g	413 (0)	400 (0)	b_u	2110 (2806)	2034 (1857)
a_g	426 (0)	416 (0)	a_g	2163 (0)	2072 (0)

[a] Ref 5. [b] Ref 4.

Table 4

A. Harmonic Vibrational Frequencies (in cm^{-1}) and Infrared Intensities (in Parentheses, in km/mol) for Octacarbonyldiiron, Unbridged $Fe_2(CO)_8$ of Point Group Symmetry D_{2h}

	B3LYP DZP	BP86 DZP	expt.[a]		B3LYP DZP	BP86 DZP	expt.[a]
b_{1g}	39*i*	61*i*		b_{3u}	437 (65)	447 (37)	
a_u	30*i*	28*i*		b_{2g}	455 (0	468 (0)	
b_{1u}	15*i*	12*i*		a_g	467 (0)	486 (0)	
b_{2g}	29 (0)	26 (0)		b_{3u}	470 (95)	502 (15)	
b_{3u}	59 (1)	62 (0)		b_{1u}	473 (19)	488 (6)	
a_g	73 (0)	73 (0)		b_{2u}	537 (76)	545 (54)	
a_u	91 (0)	86 (0)		b_{3g}	543 (0)	525 (0)	
b_{3g}	91 (0)	86 (0)		a_g	549 (0)	547 (0)	
b_{2u}	93 (1)	89 (0)		b_{1g}	556 (0)	564 (0)	
b_{2g}	97 (0)	96 (0)		a_u	556 (0)	542 (0)	
b_{1u}	102 (1)	96 (0)		b_{2g}	586 (0)	603 (0)	
b_{1g}	105 (0)	101 (0)		b_{1g}	600 (0)	586 (0)	
b_{3u}	123 (0)	119 (1)		b_{2u}	605 (49)	585 (47)	
b_{2u}	184 (0)	177 (0)		b_{1u}	615 (135)	609 (112)	
a_g	185 (0)	180 (0)		a_g	628 (0)	617 (0)	
a_g	189 (0)	183 (0)		b_{3u}	647 (369)	640 (324)	
b_{1u}	366 (1)	361 (1)		b_{1g}	2030 (0)	1949 (0)	
b_{3u}	374 (8)	402 (0)		b_{3u}	2042 (331)	1969 (29)	1974 w
b_{3g}	382 (0)	378 (0)		b_{2u}	2064 (2459)	1984 (2003)	1978 w
b_{2g}	385 (0)	379 (0)		b_{2g}	2077 (0)	1988 (0)	
a_u	402 (0)	399 (0)		a_g	2079 (0)	1997 (0)	
b_{1g}	404 (0)	400 (0)		b_{1u}	2084 (1856)	1994 (1607)	2006 s
b_{2u}	423 (0)	419 (0)		b_{3u}	2096 (2908)	2023 (2050)	2038 s
a_g	423 (2)	433 (0)		a_g	2158 (0)	2069 (0)	

B. Harmonic Vibrational Frequencies (in cm^{-1}) and Infrared Intensities (in Parentheses, in km/mol) for the Low Energetically Lying (C_{2h} Symmetry) Octacarbonyldiiron, Distorted Unbridged $Fe_2(CO)_8$

	B3LYP DZP	BP86 DZP	expt.[a]		B3LYP DZP	BP86 DZP	expt.[a]
b_u	95*i*	15*i*		a_u	415 (0)	412 ((0)	
b_u	33 (0)	54 (4)		a_g	440 (0)	445 (0)	
a_g	45 (0)	49 (0)		a_u	446 (21)	450 (7)	
a_u	54 (0)	50 (0)		b_g	448 (0)	449 (0)	
a_u	55 (0)	54 (0)		b_u	483 (1)	489 (9)	
b_g	81 (0)	77 (0)		a_g	489 (0)	491 (0)	
b_g	91 (0)	90 (0)		a_g	493 (0)	498 (0)	
a_g	93 (0)	87 (0)		b_u	500 (10)	508 (3)	
b_u	94 (0)	91 (0)		b_g	513 (0)	509 (0)	
a_u	98 (2)	95 (1)		a_u	537 (41)	528 (23)	
a_g	101 (0)	99 (0)		b_u	603 (196)	603 (176)	
a_u	107 (1)	100 (1)		a_g	610 (0)	600 (0)	
b_g	117 (0)	111 (0)		b_g	615 (0)	600 (0)	
b_u	145 (0)	161 (2)		a_u	623 (76)	612 (78)	
a_g	150 (0)	184 (0)		b_u	625 (41)	620 (31)	
b_u	161 (35)	225 (27)		a_g	630 (0)	626 (0)	
a_g	193 (0)	209 (0)		a_g	1983 (0)	1895 (0)	
a_g	302 (0)	294 (0)		b_u	1997 (1193)	1901 (842)	1974 w
b_g	351 (0)	351 (0)		b_g	2063 (0)	1971 (0)	
a_u	382 (0)	377 (0)		b_u	2067 (831)	1985 (584)	1978 w
b_u	392 (29)	402 (21)		a_g	2071 (0)	1990 (0)	
b_u	401 (8)	423 (6)		b_u	2087 (2524)	1998 (2089)	2006 s
a_g	410 (0)	425 (0)		a_u	2090 (2424)	2015 (2114)	2038 s
b_g	413 (0)	414 (0)		a_g	2157 (0)	2068 (0)	

C. Harmonic Vibrational Frequencies (in cm^{-1}) and Infrared Intensities (in parentheses, in km/mol) for C_{2h} Octacarbonyldiiron, Unbridged $Fe_2(CO)_8$

	B3LYP DZP	BP86 DZP		B3LYP DZP	BP86 DZP
b_g	254*i*	198*i*	a_g	398 (0)	404 (0)
a_u	96*i*	87*i*	b_u	407 (14)	427 (14)
b_g	37*i*	39*i*	a_u	410 (2)	407 (2)
a_u	42 (0)	44 (0)	b_g	483 (0)	490 (0)
a_g	58 (0)	53 (0)	a_g	485 (0)	499 (0)
b_u	59 (1)	56 (0)	b_u	486 (2)	500 (12)
a_u	73 (0)	69 (0)	a_g	521 (0)	525 (0)
b_u	78 (6)	81 (2)	a_g	537 (0)	528 (0)
a_g	84 (0)	80 (0)	a_u	541 (37)	549 (14)
b_g	98 (0)	95 (0)	b_u	550 (4)	539 (0)
a_u	103 (0)	99 (0)	b_u	557 (193)	564 (224)
a_g	104 (0)	102 (0)	a_g	563 (0)	564 (0)
b_u	105 (2)	100 (2)	b_g	588 (0)	599 (0)

Table 4 (Continued)

C. Harmonic Vibrational Frequencies (in cm^{-1}) and Infrared Intensities (in parentheses, in km/mol) for C_{2h} Octacarbonyldiiron, Unbridged $Fe_2(CO)_8$

	B3LYP DZP	BP86 DZP		B3LYP DZP	BP86 DZP
a_g	111 (0)	104 (0)	a_u	593 (55)	589 (56)
b_u	115 (0)	112 (0)	b_u	612 (210)	613 (111)
a_g	178 (0)	183 (0)	a_g	625 (0)	621 (0)
b_g	183 (0)	190 (0)	b_g	2037 (0)	1958 (0)
a_u	299 (4)	297 (2)	b_u	2038 (629)	1970 (21)
b_g	333 (0)	342 (0)	a_g	2056 (0)	1977 (0)
b_u	347 (123)	378 (22)	a_u	2058 (1698)	1976 (1457)
b_g	371 (0)	366 (0)	b_u	2074 (3002)	1994 (2281)
a_g	372 (0)	377 (0)	a_g	2082 (0)	1994 (0)
a_u	374 (0)	366 (0)	b_u	2090 (2335)	2012 (1966)
b_u	395 (9)	392 (20)	a_g	2153 (0)	2064 (0)

D. Harmonic Vibrational Frequencies (in cm^{-1}) and Infrared Intensities (in parentheses, in km/mol) for D_{2d} Octacarbonyldiiron, Unbridged $Fe_2(CO)_8$

	B3LYP DZP	BP86 DZP		B3LYP DZP	BP86 DZP
b_2	49*i*	25 (48)	b_2	410 (2)	434 (0)
e	22*i*	10 (0)	e	427 (0)	430 (3)
b_1	8*i*	10*i*	e	445 (28)	454 (8)
a_1	52 (0)	58 (0)	a_1	453 (0)	461 (0)
e	56 (0)	62 (0)	b_2	455 (2)	451 (27)
a_1	67 (0)	80 (0)	a_1	478 (0)	497 (0)
b_2	69 (1)	79 (0)	b_2	506 (22)	510 (41)
e	76 (1)	73 (0)	a_1	529 (0)	536 (0)
a_2	92 (0)	87 (0)	a_2	576 (0)	557 (0)
b_1	93 (0)	89 (0)	b_1	580 (0)	562 (0)
e	93 (1)	89 (0)	e	616 (59)	614 (53)
a_1	103 (0)	131 (0)	e	637 (60)	641 (47)
b_2	319 (466)	360 (343)	e	2029 (234)	1941 (157)
e	342 (4)	339 (3)	a_1	2059 (0)	1973 (0)
e	348 (0)	349 (1)	b_2	2065 (2071)	1984 (1538)
a_2	356 (0)	360 (0)	e	2070 (2386)	1980 (1994)
b_1	357 (0)	360 (0)	b_2	2099 (459)	2007 (619)
a_1	408 (0)	428 (0)	a_1	2154 (0)	2067 (0)

[a] Refs 5 and 6.

discovery of the lower energy distorted dibridged C_{2v} structure reported in Figure 9b. This C_{2v} $Fe_2(CO)_6$ structure, our lowest energy $Fe_2(CO)_6$ structure, lies 12.1−13.2 kcal/mol (B3LYP) or 16.0−16.4 kcal/mol (BP86) below the quadruple bond unbridged structure. Our second lowest energy $Fe_2(CO)_6$ structure is the C_{2v} dibridged structure of Figure 9c, which lies 5.6 kcal/mol (B3LYP) or 3.1 kcal/mol (BP86) above Figure 9b.

On a per CO bond basis, the dissociation energies in Table 1 are remarkably uniform, with the B3LYP results ranging from 26.5 to 31.3 kcal/mol, when the high energy quadruply bridged structure of $Fe_2(CO)_8$ is excluded. An alternate, more sensitive way of looking at the thermochemical results is in terms of the single carbonyl removal reactions

$$Fe_2(CO)_x \rightarrow Fe_2(CO)_{x-1} + CO \qquad (8)$$

and these results are seen in Table 2. As noted in the Introduction, there is an experimental value[16] for the extrusion of CO from $Fe_2(CO)_9$, namely 28 kcal/mol. Our DZP B3LYP prediction of 29.4 kcal/mol is in good agreement. Our DZP BP86 value of 34.2 kcal/mol for $D_e[Fe_2(CO)_8\cdots CO]$ is somewhat above the Russian experiment, and slightly higher than the very recent DFT prediction of 32.3 kcal/mol by Barckholtz and Bursten.[15]

Comparison of the predictions of Table 2 with the radical cation experimental results of Markin and Sugawara,[17] eqs 1, 2, and 3 in our introduction, is of interest. It is seen that the neutral $Fe_2(CO)_x$ compounds have significantly larger dissociation energies for CO removal than do the analogous radical cations. In particular, the radical cation $Fe_2(CO)^+_8$ loses a carbonyl very easily, $D_e[Fe_2(CO)^+_7\cdots CO] = 7.6$ kcal. For the analogous neutral system, this dissociation energy is predicted to be three times larger, namely 25.4 kcal/mol. So it would seem that there are major differences between the neutral $Fe_2(CO)_x$ and radical cation $Fe_2(CO)^+_x$ systems.

C. Vibrational Frequencies. Harmonic vibrational frequencies have been evaluated for all structures described above and are reported in Tables 3−13. Our discussion turns first to the question of whether the geometries optimized are in fact genuine minima. It must be stated at the outset that low-magnitude imaginary vibrational frequencies are suspect with all currently available DFT methods. This is because the numerical integration procedures used in modern DFT methods have significant limitations. Thus, when we see an imaginary vibrational frequency of magnitude less than $100i$ cm^{-1}, we conclude only that there is a genuine minimum of energy identical to or very close to the stationary point in question. We do not follow the imaginary eigenvector in search of a stationary point with no imaginary vibrational frequencies. If one cannot live with this sort of uncertainty, one should not be using DFT methods on systems the size of $Fe_2(CO)_9$ in the year 2000. Of course we hope that future DFT developments will yield more accurate predictions for low fundamental vibrational frequencies. The above limitations notwithstanding, in several $Fe_2(CO)_x$ cases we pursued very large integration grids, and a few of these results will be noted below.

With respect to the $Fe_2(CO)_8$ vibrational frequencies, it is unambiguous that the dibridged D_{2h} structure (Figure 2) is a

Table 5. Harmonic Vibrational Frequencies (in cm^{-1}) and Infrared Intensities (in Parentheses, in km/mol) for Tetra-μ-carbonyltetracarbonyldiiron, Tetrabridged $Fe_2(CO)_8$

	B3LYP DZP	BP86 DZP
b_1	367*i*	316*i*
b_2	307*i*	146*i*
a_u	171*i*	102*i*
b_3	106*i*	44*i*
b_2	45 (1)	38 (1)
b_1	73 (1)	66 (1)
a_u	85 (0)	96 (0)
b_1	86 (0)	77 (0)
a_g	93 (0)	87 (0)
b_3	100 (0)	95 (0)
b_2	101 (3)	97 (1)
b_2	103 (0)	99 (0)
a_g	104 (0)	99 (0)
b_1	115 (0)	112 (0)
b_3	160 (0)	196 (0)
b_3	194 (0)	235 (0)
a_u	219 (0)	234 (0)
a_g	267 (0)	261 (0)
b_2	268 (0)	272 (0)
b_1	278 (0)	268 (0)
b_2	349 (32)	367 (3)
a_g	353 (0)	371 (0)
b_3	361 (0)	357 (0)
b_3	375 (0)	362 (0)
b_3	375 (1)	380 (0)
b_1	385 (3)	396 (1)
b_2	409 (41)	404 (28)
b_1	429 (0)	431 (0)
b_2	439 (60)	453 (34)
a_u	450 (0)	442 (0)
b_1	487 (0)	449 (0)
b_3	518 (159)	529 (80)
b_2	520 (0)	498 (0)
a_g	533 (0)	524 (0)
b_1	534 (36)	530 (26)
b_1	535 (0)	529 (0)
b_3	562 (112)	544 (75)
b_2	570 (93)	571 (112)
a_g	600 (0)	570 (0)
a_g	614 (0)	603 (0)
b_3	1917 (0)	1858 (0)
b_2	1936 (1429)	1866 (1019)
b_1	1962 (1255)	1877 (1046)
a_g	1964 (0)	1879 (0)
b_1	2085 (0)	1996 (0)
b_2	2085 (1285)	1996 (1101)
b_3	2096 (3079)	2013 (2546)
a_g	2146 (0)	2055 (0)

Table 6. Harmonic Vibrational Frequencies (in cm^{-1}) and Infrared Intensities (in Parentheses, in km/mol) for Mono-μ-carbonylhexacarbonyldiiron, Monobridged $Fe_2(CO)_7$

	B3LYP DZP	BP86 DZP
b_2	490*i*	487*i*
b_1	72*i*	82*i*
b_2	70*i*	31*i*
a_2	64*i*	61*i*
b_1	56 (0)	50 (0)
a_1	70 (1)	65 (1)
a_2	77 (0)	75 (0)
a_1	82 (1)	80 (0)
b_1	90 (0)	87 (0)
b_2	96 (3)	96 (2)
a_2	100 (0)	102 (0)
b_2	103 (2)	100 (3)
a_1	109 (0)	100 (0)
b_2	194 (17)	195 (13)
a_1	274 (1)	271 (1)
b_1	325 (0)	313 (1)
b_2	331 (48)	369 (52)
a_2	336 (0)	331 (0)
a_1	345 (3)	356 (1)
b_1	368 (0)	365 (0)
a_1	412 (1)	411 (1)
a_2	412 (0)	423 (0)
b_2	449 (0)	458 (10)
b_1	458 (12)	441 (25)
a_1	466 (0)	477 (0)
b_2	476 (4)	482 (8)
a_2	480 (0)	476 (0)
b_1	484 (53)	500 (17)
a_1	535 (19)	536 (3)
a_2	538 (0)	562 (0)
b_1	555 (53)	551 (51)
b_2	561 (281)	564 (203)
a_1	577 (58)	581 (66)
a_1	585 (25)	584 (18)
b_2	601 (9)	608 (2)
b_2	2040 (313)	1969 (12)
a_2	2065 (0)	1974 (0)
a_1	2072 (1727)	1975 (746)
b_1	2075 (1897)	1985 (1615)
a_1	2081 (352)	1990 (1030)
b_2	2087 (2218)	2009 (1643)
a_1	2147 (5)	2052 (6)

genuine minimum with both the B3LYP and BP86 methods. The unbridged $Fe_2(CO)_8$ structure has three very small imaginary vibrational frequencies (39*i*, 30*i*, 15*i* cm^{-1}, B3LYP), indicating that this structure is either a minimum or very close energetically to a minimum. The distorted D_{2h} unbridged $Fe_2(CO)_8$ has only one imaginary vibrational frequency (95*i* cm^{-1}, B3LYP; 15*i* cm^{-1}, BP86), and we conclude from its lower (than D_{2h}) energy that the C_{2h} structure is probably a genuine minimum. The quadruply bridged $Fe_2(CO)_8$ structure has several imaginary frequencies in magnitude above 100*i* cm^{-1}, including the b_1 frequency at 367*i* (B3LYP) or 316*i* cm^{-1} (BP86). Clearly, the quadruply bridged $Fe_2(CO)_8$ structure is not a genuine minimum. Because this structure is also very high-lying energetically (see Table 1) we need consider it no further.

For $Fe_2(CO)_7$ the lower energy triply bridged structure has one imaginary vibrational frequency at 90*i* cm^{-1} (B3LYP) or 67*i* cm^{-1} (BP86). We interpret this small vibrational frequency as due to numerical roundoff and assume that our triply bridged structure is a genuine minimum or very close to a genuine minimum. However, the higher energy monobridged structure (Figure 5) has a substantial imaginary vibrational frequency, 490*i* (B3LYP) or 487*i* cm^{-1} (BP86). Therefore we conclude that while our C_{2v} symmetry monobridged $Fe_2(CO)_7$ is close to a minimum, it is probably not a genuine minimum. Table 8 makes it clear that our lowest energy $Fe_2(CO)_7$ structure, the distorted unbridged Figure 7, is a genuine minimum.

Turning last to the stationary points of $Fe_2(CO)_6$, Table 9 shows that the unbridged structure, with a very short (possibly quadruple) iron−iron bond, is a minimum (or trivially close to a minimum) with both the B3LYP and BP86 methods. However, the dibridged structure (Table 10a), with a much longer iron−iron bond, appears not to be a genuine minimum. The imaginary vibrational frequency at 414*i* cm^{-1} (B3LYP) or 389*i* cm^{-1} (BP86) appears to point toward a lower energy minimum than that of the dibridged structure seen in Figure 9a. That lower energy structure is seen in Figure 9b, with its vibrational frequencies reported in Table 10b. The latter table shows the distorted dibridged structure of C_{2h} symmetry to be a genuine minimum with the DZP B3LYP method and to have a single low imaginary frequency (33*i* cm^{-1}) with DZP BP86.

For the quadruple bond $Fe_2(CO)_6$ structure, we have pursued the possibly fictitious small imaginary vibrational frequencies. Table 9 shows the a_{1g} vibrational frequency for this structure

Table 7. Harmonic Vibrational Frequencies (in cm^{-1}) and Infrared Intensities (in Parentheses, in km/mol) for Tri-μ-carbonyltetracarbonyldiiron, Tribridged $Fe_2(CO)_7$

	B3LYP DZP	BP86 DZP
a_2	90*i*	67*i*
b_2	8 (0)	19 (0)
b_2	68 (0)	65 (0)
a_1	73 (1)	71 (0)
a_2	77 (0)	111 (0)
b_1	81 (10)	90 (0)
a_1	91 (1)	87 (1)
b_2	95 (1)	92 (1)
a_1	100 (0)	98 (0)
b_1	100 (10)	106 (0)
b_1	109 (4)	179 (1)
a_2	117 (0)	146 (0)
b_1	176 (0)	191 (19)
b_1	270 (7)	294 (10)
a_1	274 (0)	275 (0)
a_2	276 (0)	287 (0)
b_1	312 (0)	326 (0)
b_2	354 (4)	359 (3)
a_2	363 (0)	347 (0)
b_2	371 (1)	366 (0)
b_2	377 (1)	388 (2)
a_1	386 (2)	395 (1)
a_1	396 (6)	412 (2)
b_2	460 (6)	472 (0)
a_2	460 (0)	474 (0)
b_1	472 (55)	496 (6)
b_2	486 (1)	490 (0)
a_1	490 (5)	489 (3)
a_1	521 (0)	530 (0)
b_2	564 (114)	569 (95)
a_2	576 (0)	585 (0)
b_1	584 (24)	581 (37)
a_1	612 (35)	612 (28)
b_1	626 (55)	616 (49)
a_1	643 (0)	638 (0)
a_1	1992 (828)	1910 (1100)
a_1	2004 (506)	1916 (8)
b_2	2010 (823)	1914 (676)
a_2	2071 (0)	1982 (0)
b_2	2074 (1531)	1986 (1199)
b_1	2088 (2766)	2009 (2223)
a_1	2140 (0)	2049 (0)

Table 8. Harmonic Vibrational Frequencies (in cm^{-1}) and Infrared Intensities (in Parentheses, in km/mol) for the (C_s Symmetry) Heptacarbonyldiiron, $Fe_2(CO)_7$ with Two Highly Unsymmetrical Bridging Carbonyls; This is the Energetically Lowest Lying $Fe_2(CO)_7$ Structure

	B3LYP DZP	BP86 DZP
a″	13 (0)	5 (0)
a″	41 (0)	44 (0)
a′	60 (1)	56 (1)
a″	74 (0)	65 (0)
a′	76 (1)	69 (1)
a″	77 (0)	73 (0)
a′	78 (1)	76 (1)
a″	83 (0)	79 (0)
a′	97 (0)	89 (2)
a″	99 (0)	96 (0)
a′	101 (0)	95 (0)
a′	107 (2)	98 (1)
a′	129 (0)	128 (0)
a′	238 (0)	233 (0)
a″	369 (0)	370 (0)
a′	370 (3)	356 (3)
a″	372 (0)	373 (0)
a″	385 (2)	380 (0)
a′	398 (54)	400 (41)
a″	400 (0)	399 (0)
a′	419 (1)	416 (2)
a′	439 (41)	467 (13)
a′	447 (3)	435 (9)
a″	460 (1)	461 (1)
a′	473 (13)	481 (26)
a′	492 (15)	500 (4)
a″	496 (1)	494 (1)
a′	509 (19)	517 (15)
a″	509 (2)	522 (4)
a′	539 (50)	547 (32)
a″	548 (108)	564 (77)
a′	598 (134)	595 (112)
a″	602 (7)	619 (12)
a′	611 (108)	612 (86)
a′	627 (52)	623 (45)
a′	2011 (1107)	1930 (651)
a′	2032 (101)	1967 (20)
a″	2066 (95)	1974 (192)
a″	2079 (1795)	1988 (1436)
a′	2083 (1067)	1987 (958)
a′	2095 (2109)	2013 (1640)
a′	2146 (31)	2053 (46)

to be 18*i* cm^{-1} with B3LYP and 11*i* cm^{-1} with BP86. As discussed in the Theoretical Methods section, these results were obtained with the (75 302) fine grid in the Gaussian 94 program.[26] For the $Fe_2(CO)_6$ structure of Figure 8, we reoptimized the B3LYP geometry with the ultrafine (99 590) numerical integration grid. The new B3LYP is essentially unchanged, with the Fe—Fe distance moving from 2.0025 to 2.0026 Å. The new B3LYP a_{1g} vibrational frequency is 17*i* cm^{-1}. We remain unconvinced (see earlier discussion in Theoretical Methods section) that this imaginary vibrational frequency is genuine. If the 17*i* cm^{-1} is genuine, it means that a true $Fe_2(CO)_6$ minimum energy geometry is extremely close to the D_{3d} structure seen in Figure 8. Thus, for all practical purposes, the geometry seen in Figure 8 is the true structure.

For both the dibridged and unbridged structures of $Fe_2(CO)_8$, Poliakoff, Turner, and Fletcher[4,5] have reported experimental fundamentals. These are included in plausible relationship to the theoretical predictions in Tables 3 and 4. We turn first to the dibridged $Fe_2(CO)_8$ structure, seen in Figure 2. Fletcher, Poliakoff, and Turner[5] note that their observed vibrational features at 2022, 2032, and 2055 cm^{-1} fall in the terminal C—O stretching region near 2000 cm^{-1}. The present theoretical BP86 frequencies fit well with these three experimental features (differences 16, 31, and 25 cm^{-1}, respectively), and all three fundamentals are predicted to have very large IR intensities. The B3LYP frequencies also agree qualitatively with the three observed fundamentals, but with larger differences, namely 70, 62, and 51 cm^{-1}.

The two observed vibrational frequencies at 1814 and 1857 (weak) cm^{-1} are stated by Fletcher, Poliakoff, and Turner to fall in the bridging C—O stretching region near 1840 cm^{-1}. The present BP86 predictions for the D_{2h} symmetry dibridged $Fe_2(CO)_6$ appear to agree well with the observed features, falling 27 and 13 cm^{-1} above the experimental results. Also, the feature labeled "weak" by Fletcher, Poliakoff, and Turner[5] does have by far the smallest theoretical IR intensity (148 km/mole) of the five reported fundamentals.

Fletcher, Poliakoff, and Turner[5] also assigned four fundamentals to the unbridged structure (Figure 3a) of $Fe_2(CO)_8$. All four observed features fall above the 1840 cm^{-1} range conventionally associated with bridging C—O stretches. Similarly, the theoretical methods predict no fundamentals near 1840 cm^{-1} for the unbridged $Fe_2(CO)_8$. The agreement between DZP BP86 and experiment is good, the differences being −5, +6, −12, and −15 cm^{-1}. However, there seems to be an inconsistency with respect to the IR intensities. Fletcher labels two of the IR

Table 9. Harmonic Vibrational Frequencies (in cm^{-1}) and Infrared Intensities (in Parentheses, in km/mol) for Hexacarbonyldiiron, Unbridged $Fe_2(CO)_6$ of D_{3h} and D_{3d} Symmetry

	D_{3h}			D_{3d}	
	B3LYP DZP	BP86 DZP		B3LYP DZP	BP86 DZP
a_1''	15 (0)	12 (0)	a_{1g}	18*i*	11*i*
e'	44 (0)	40 (0)	e_u	6 (1)	8*i*
a_2''	55 (1)	48 (2)	a_{2u}	42 (0)	30 (2)
e''	62 (0)	63 (0)	e_g	71 (0)	71 (0)
a_1'	75 (0)	74 (0)	a_{1g}	72 (0)	70 (0)
e'	84 (0)	82 (0)	e_u	76 (0)	75 (0)
e''	126 (0)	120 (0)	e_g	126 (0)	121 (0)
a_1'	312 (0)	301 (0)	e_u	292 (5)	290 (1)
a_2''	342 (2)	321 (2)	a_{1g}	313 (0)	302 (0)
e'	342 (0)	332 (0)	a_{2u}	331 (5)	310 (0)
a_2'	365 (0)	361 (0)	a_{1u}	350 (0)	350 (0)
a_1''	381 (0)	374 (0)	a_{2g}	368 (0)	364 (0)
e''	382 (0)	391 (0)	e_g	404 (0)	408 (0)
e''	452 (0)	449 (0)	e_u	447 (1)	442 (2)
a_1'	462 (0)	470 (0)	a_{1g}	455 (0)	463 (0)
a_2''	479 (74)	505 (20)	a_{2u}	476 (79)	503 (23)
e'	485 (20)	498 (4)	e_g	486 (0)	496 (0)
e''	562 (0)	582 (0)	e_u	537 (142)	558 (102)
e'	568 (123)	570 (99)	a_{1g}	586 (0)	588 (0)
a_1'	585 (0)	586 (0)	e_g	589 (0)	595 (0)
e''	2062 (0)	1970 (0)	e_g	2063 (0)	1972 (0)
e'	2070 (2017)	1977 (1713)	e_u	2068 (2062)	1975 (1742)
a_2''	2076 (2436)	1996 (1860)	a_{2u}	2074 (2397)	1994 (1834)
a_1'	2147 (0)	2051 (0)	a_{1g}	2146 (0)	2050 (1)

features as strong and the other two as "rather weak". For the unbridged structure of Figure 3b, we predict three strong and one weak IR fundamental with both B3LYP and BP86 methods.

As predicted earlier by Jacobsen and Ziegler,[14] the distorted unbridged C_{2h} structure of $Fe_2(CO)_8$ is confirmed here to lie below the D_{2h} structure assumed by experiment.[4,5] For this C_{2h} symmetry structure, we do find two higher C−O stretches (2087 and 2090 cm^{-1}, B3LYP) with very large IR intensities and two lower carbonyl stretches (1997 and 2067 cm^{-1}, B3LYP) with weaker IR intensities. The agreement between theory and experiment is +23, +85, +81, and +52 cm^{-1} for B3LYP and −73, +7, −8, and −23 cm^{-1} for BP86. Our results are qualitatively similar to those reported earlier by Jacobsen and Ziegler,[14] and we support their conclusion that the IR intensities appear to favor the distorted unbridged C_{2h} symmetry structure.

Finally, we turn to the question of iron−iron bonding as reflected in the theoretical vibrational frequencies. Note that although several Fe−Fe multiply bonded systems have been characterized structurally, there are apparently no experimentally known Fe−Fe multiply bonded stretching frequencies.[2] In part this is due to the low IR intensities associated with the Fe−Fe stretching motion (See Tables 3−13). The present Fe−Fe stretching analysis was carried out in terms of the potential energy distributions (PEDs) evaluated using the remarkable program INTDER developed by Wesley D. Allen and co-workers. Assuming sets of standard internal coordinates, the PEDs pertaining to the iron−iron stretch are reported in Table 14. The lowest frequency (73 cm^{-1}) to contribute significantly (12%) to any Fe−Fe stretching motion occurs for the unbridged D_{2h} structure of $Fe_2(CO)_8$, Figure 3a. The highest frequency (643 cm^{-1}) to contribute significantly (10%) to any stretching motion occurs for the tribridged structure of $Fe_2(CO)_7$, Figure 6.

Let us focus now on the lowest energy structure of each $Fe_2(CO)_x$ species. For $Fe_2(CO)_8$, the Fe−Fe stretch in the dibridged structure is dominated by the predicted harmonic vibrational frequency at 231 cm^{-1} (79%). On structural grounds, we classify

Table 10

A. Harmonic Vibrational Frequencies (in cm^{-1}) and Infrared Intensities (in Parentheses, in km/mol) for Di-μ-carbonyltetracarbonyldiiron,Dibridged $Fe_2(CO)_6$ of Point Group Symmetry D_{2h}

	B3LYP DZP	BP86 DZP		B3LYP DZP	BP86 DZP
b_{2g}	414*i*	389*i*	b_{3u}	368 (5)	393 (0)
b_{1u}	202*i*	235*i*	b_{3g}	398 (0)	396 (0)
b_{3g}	65*i*	44 (0)	b_{2u}	411 (42)	420 (38)
b_{2u}	23 (0)	19 (0)	a_g	436 (0)	442 (0)
a_u	40 (0)	44 (0)	b_{3u}	475 (81)	516 (56)
b_{1g}	59 (0)	52 (0)	b_{2g}	479 (0)	477 (0)
b_{3u}	59 (0)	68 (0)	a_g	490 (0)	487 (0)
a_g	71 (0)	70 (0)	b_{1g}	498 (0)	501 (0)
b_{2g}	92 (0)	96 (0)	b_{1u}	506 (0)	522 (0)
b_{2u}	105 (6)	98 (4)	a_g	572 (0)	582 (0)
b_{3g}	160 (0)	249 (0)	b_{2u}	584 (41)	581 (27)
b_{1u}	169 (0)	154 (0)	b_{3u}	697 (151)	694 (124)
b_{3u}	202 (13)	202 (4)	b_{1u}	1863 (1122)	1796 (820)
a_g	275 (0)	277 (0)	a_g	1874 (0)	1811 (0)
b_{2g}	292 (0)	283 (0)	b_{1g}	2063 (0)	1955 (0)
b_{2u}	352 (16)	347 (11)	b_{2u}	2080 (2276)	1974 (2032)
a_u	353 (0)	357 (0)	b_{3u}	2091 (2378)	1996 (1746)
b_{1g}	357 (0)	356 (0)	a_g	2141 (0)	2036 (0)

B. Harmonic Vibrational Frequencies (in cm^{-1}) and Infrared Intensities (in Parentheses, in km/mol) for the (C_{2h} Symmetry) Di-μ-carbonyltetra−Carbonyldiiron, Trans Dibridged $Fe_2(CO)_6$; This is the Lowest Energy Structure Predicted for $Fe_2(CO)_6$

	B3LYP DZP	BP86 DZP		B3LYP DZP	BP86 DZP
b_g	28 (0)	33*i*	a_g	432 (0)	433 (0)
a_u	28 (0)	25 (0)	b_u	438 (17)	434 (12)
a_u	53 (0)	50 (0)	a_g	476 (0)	478 (0)
b_u	75 (1)	70 (0)	a_u	480 (37)	498 (17)
a_g	77 (0)	75 (0)	b_u	485 (44)	522 (9)
b_u	80 (0)	80 (0)	a_g	520 (0)	514 (0)
a_g	86 (0)	87 (0)	b_g	520 (0)	545 (0)
b_g	90 (0)	84 (0)	b_u	584 (50)	591 (41)
a_u	124 (1)	112 (1)	a_u	585 (57)	583 (43)
b_u	146 (8)	153 (6)	a_g	591 (0)	583 (0)
a_g	197 (0)	195 (0)	a_g	598 (0)	600 (0)
a_g	256 (0)	255 (0)	b_u	644 (289)	650 (273)
b_g	301 (0)	301 (0)	b_u	1858 (1037)	1811 (831)
a_u	356 (3)	352 (2)	a_g	1887 (0)	1828 (0)
a_u	390 (4)	384 (2)	b_g	2072 (0)	1970 (0)
b_u	395 (2)	400 (1)	a_u	2081 (1954)	1981 (1686)
b_g	396 (0)	385 (0)	b_u	2094 (2513)	2000 (1873)
b_g	420 (0)	429 (0)	a_g	2134 (0)	2034 (0)

C. Harmonic Vibrational Frequencies (in cm^{-1}) and Infrared Intensities (in Parentheses, in km/mol) for C_{2v} Di-μ-tetracarbonyldiiron, Dibridged $Fe_2(CO)_6$

	B3LYP DZP	BP86 DZP		B3LYP DZP	BP86 DZP
b_1	27 (0)	25 (0)	a_2	429 (0)	431 (0)
a_2	30 (0)	27 (0)	a_1	437 (2)	437 (1)
b_2	63 (1)	69 (0)	b_1	454 (37)	459 (5)
a_1	72 (1)	71 (1)	b_2	464 (5)	465 (0)
b_2	77 (2)	78 (1)	b_1	470 (6)	469 (16)
b_1	79 (0)	78 (0)	a_1	475 (2)	491 (0)
a_1	79 (1)	78 (1)	b_2	517 (60)	523 (14)
a_2	89 (0)	84 (0)	a_2	519 (0)	544 (0)
b_1	102 (2)	98 (2)	a_1	550 (2)	555 (1)
b_2	174 (5)	173 (3)	b_1	592 (55)	588 (42)
a_1	252 (0)	256 (0)	a_1	596 (26)	601 (17)
b_2	252 (1)	257 (0)	b_2	652 (76)	625 (80)
b_2	333 (2)	348 (1)	a_1	1879 (105)	1821 (85)
b_1	345 (2)	346 (2)	a_1	1892 (1183)	1833 (910)
a_2	367 (0)	362 (0)	a_2	2066 (0)	1965 (0)
b_1	381 (1)	374 (0)	b_1	2077 (2008)	1976 (1743)
a_1	396 (0)	399 (0)	b_2	2087 (2458)	1994 (1824)
b_2	428 (10)	435 (0)	a_1	2137 (116)	2036 (85)

This is the lowest energy structure predicted for $Fe_2(CO)_6$.

Table 11. Harmonic Vibrational Frequencies (in cm^{-1}) and Infrared Intensities (in Parentheses, in km/mol) for C_{2v} Hexacarbonyldiiron, Unsymmetrical Unbridged $Fe_2(CO)_6$

	B3LYP DZP	BP86 DZP
a_2	54*i*	82*i*
a_2	16 (0)	26 (0)
b_2	21 (1)	19*i*
b_1	23 (0)	14 (0)
b_2	58 (0)	48 (0)
a_1	84 (0)	84 (0)
b_1	93 (0)	89 (0)
a_1	97 (0)	93 (0)
b_2	103 (1)	96 (1)
a_1	105 (5)	104 (1)
b_1	125 (1)	128 (1)
a_1	224 (0)	240 (0)
a_2	329 (0)	284 (0)
a_2	369 (0)	371 (0)
b_2	369 (3)	359 (2)
a_2	374 (0)	390 (0)
b_1	384 (4)	377 (2)
b_2	396 (0)	403 (0)
a_1	413 (5)	435 (4)
b_1	430 (28)	452 (15)
a_2	439 (0)	448 (0)
b_2	457 (12)	473 (5)
a_1	490 (58)	523 (6)
b_1	495 (0)	503 (0)
a_1	553 (11)	546 (0)
b_2	556 (41)	588 (24)
a_1	566 (0)	558 (2)
b_1	622 (33)	614 (30)
b_2	626 (47)	620 (42)
a_1	674 (23)	677 (7)
b_2	2014 (543)	1930 (441)
a_1	2026 (2877)	1961 (1563)
b_1	2063 (1525)	1978 (1261)
b_2	2067 (1834)	1980 (1419)
a_2	2075 (0)	1992 (0)
a_1	2141 (47)	2055 (75)

Table 12. Harmonic Vibrational Frequencies (in cm^{-1}) and Infrared Intensities (in Parentheses, in km/mol) for C_{2v} Hexacarbonyldiiron, Distorted Unbridged $Fe_2(CO)_6$

	B3LYP DZP	BP86 DZP
b_1	374*i*	63*i*
b_2	11*i*	27 (0)
a_2	43 (0)	37 (0)
b_1	54 (1)	16*i*
b_2	62 (0)	32 (0)
a_1	69 (0)	48 (3)
a_1	74 (0)	86 (0)
a_2	78 (0)	83 (0)
b_1	92 (0)	127 (0)
b_2	106 (0)	84 (1)
a_1	107 (0)	111 (0)
a_1	210 (6)	246 (9)
b_1	224 (0)	270 (7)
a_2	339 (0)	348 (0)
b_1	358 (7)	379 (3)
b_2	360 (1)	333 (0)
a_2	397 (0)	392 (0)
a_1	407 (0)	385 (4)
b_2	414 (3)	394 (0)
a_1	419 (32)	412 (19)
a_1	454 (5)	419 (13)
b_2	463 (0)	461 (0)
a_1	476 (82)	488 (16)
b_1	488 (0)	434 (0)
b_2	500 (55)	565 (57)
a_1	501 (43)	520 (3)
a_2	506 (0)	541 (0)
b_2	560 (71)	577 (18)
a_1	597 (24)	656 (2)
b_1	601 (126)	526 (36
b_1	1989 (1645)	1922 (1231)
a_1	2003 (43)	1929 (76)
b_2	2064 (439)	1951 (693)
b_2	2075 (1526)	1990 (1102)
a_1	2084 (2513)	1987 (1593)
a_1	2137 (40)	2036 (80)

this $Fe_2(CO)_8$ geometry (Figure 2) as a weak double bond. Our lowest energy $Fe_2(CO)_7$ structure, the distorted unbridged geometry, is dominated (81%) by a slightly higher fundamental, namely 238 cm^{-1}. This structure (Figure 7) was assigned a bond order of 5/2 in our structural discussion above. Finally, our energetically favored $Fe_2(CO)_6$ structure, the distorted dibridged geometry of Figure 8b, is dominated (86%) in terms of Fe−Fe stretching character by the fundamental predicted at 256 cm^{-1}. Because we earlier characterized this C_{2h} structure as a weak double bond, it is reasonable that its Fe−Fe stretch should fall below that for the tribridged $Fe_2(CO)_7$ structure just discussed.

The only assigned Fe$\overset{4}{—}$Fe quadruple bond in this study is the unbridged $Fe_2(CO)_6$ structures, with predicted iron−iron distance 2.00 Å. Therefore, the vibrational analysis of this structure is of special interest. In accordance in Badger's Rule, we do predict this quadruple bond species to have the highest fundamental frequency associated with the Fe−Fe stretching motion. The Fe$\overset{4}{—}$Fe stretch is dominated by 312 cm^{-1} (68%) for the D_{3h} structure or 313 cm^{-1} (68%) for the D_{3d} structure, but also has a hefty contribution (20% or 22%) from the higher frequency 585 cm^{-1} (D_{3h}) or 586 cm^{-1} (D_{3d}). The only other structure with significant high iron−iron stretching contribution (23% of the fundamental at 614 cm^{-1}) is the high-energy quadruply bridged $Fe_2(CO)_8$ structure (Figure 4).

Thus, one does observe a general correlation between iron−iron bond distances and stretching vibrational frequencies. However, there is not a clear correlation between thermodynamic stability and bond distance.

Synthetic Prospects

Loss of one or more CO groups from the established structure of $Fe_2(CO)_9$ (Figure 1) with relatively little change in the molecular geometry except for shortening the iron−iron bond as the formal metal−metal bond order is increased (Figure 13) leads to $Fe_2(CO)_x$ structures ($x = 8$, 7, and 6) corresponding to genuine minima (Figures 2, 6, and 7, respectively). However, the tribridged structure for $Fe_2(CO)_7$, although a local minimum, is of higher energy than a subsequently discovered alternative C_s structure (Figure 7) having two highly unsymmetrical carbonyl groups similar to the bridging CO configuration in the structurally characterized[36,37] $(C_5H_5)_2V_2(CO)_5$, which bears a similar relationship to the stable $C_5H_5V(CO)_4$ as $Fe_2(CO)_7$ bears to $Fe(CO)_5$. Similarly, the D_{3d} unbridged structure of $Fe_2(CO)_6$, although also a local minimum, is of higher energy than a C_{2h} dibridged structure (Figure 9b) in which there are two bridging CO groups distorted so that they can function as four-electron donors. Assuming that the iron atoms maintain the formal 18-electron configuration, the distortion of D_{3d} unbridged $Fe_2(CO)_6$ to C_{2h} dibridged $Fe_2(CO)_6$ lowers the iron−iron bond order from four to two, consistent with an increase in the computed iron−iron bond distance from 2.01 ± 0.1 to 2.43 Å.

A question of interest is whether any of the formal decarbonylation processes depicted in Figure 13 can be carried out to produce isolable quantities of homoleptic binuclear iron

(36) Cotton, F. A.; Kruczynski, L.; Frenz, B. A. *J. Organomet. Chem.* **1978**, *160*, 93.

(37) Huffman, J. C.; Lewis, L. N.; Caulton, K. G. *Inorg. Chem.* **1980**, *19*, 2755.

Table 13. Harmonic Vibrational Frequencies (in cm^{-1}) and Infrared Intensities (in Parentheses, in km/mol) for C_s Mono-μ-pentacarbonyldiiron, Monobridged $Fe_2(CO)_6$

	B3LYP DZP	BP86 DZP
a″	32*i*	31*i*
a″	44 (0)	41 (0)
a′	45 (2)	43 (1)
a″	63 (0)	59 (0)
a′	68 (1)	68 (0)
a′	78 (1)	76 (1)
a″	82 (0)	81 (0)
a′	89 (0)	88 (0)
a′	104 (0)	98 (0)
a″	106 (0)	101 (0)
a′	141 (7)	156 (1)
a′	275 (1)	288 (0)
a′	312 (2)	313 (0)
a″	342 (0)	328 (1)
a″	357 (0)	353 (0)
a″	370 (0)	367 (0)
a′	378 (8)	384 (0)
a′	416 (5)	435 (11)
a″	419 (0)	413 (0)
a′	449 (4)	445 (3)
a″	460 (0)	446 (0)
a′	468 (19)	478 (8)
a′	487 (12)	494 (5)
a′	495 (29)	504 (14)
a″	504 (1)	509 (2)
a″	524 (104)	542 (65)
a′	549 (89)	564 (60)
a″	563 (24)	586 (22)
a′	587 (27)	585 (17)
a′	603 (77)	612 (52)
a′	1992 (986)	1918 (729)
a″	2058 (433)	1963 (628)
a′	2065 (767)	1982 (725)
a″	2074 (1563)	1981 (1156)
a′	2084 (2087)	2000 (1413)
a′	2142 (98)	2049 (111)

carbonyls containing iron−iron multiple bonds. This is not a very promising possibility because $Fe_2(CO)_9$ is well known to decompose only slightly above room temperature by rupture of the iron−iron bond without carbonyl loss to give stable $Fe(CO)_5$ and a reactive coordinately unsaturated $Fe(CO)_4$ fragment by the reaction[38]

$$Fe_2(CO)_9 \rightarrow Fe(CO)_5 + Fe(CO)_4 \qquad (9)$$

This suggests that the Fe−Fe bond in $Fe_2(CO)_9$ may be more readily broken than the Fe−CO bonds, so that the prospects for carrying out any of the decarbonylation reactions in Figure 13 in gram quantities are unpromising.

The prospect for synthesizing binuclear iron carbonyl derivatives containing iron−iron multiple bonds can be improved if some of the carbonyl groups are replaced by other ligands, thereby suppressing elimination of $Fe(CO)_5$ by eq 9 leading to rupture of the iron−iron bond. Of particular interest are some reported and structurally characterized binuclear cyclobutadiene iron carbonyl complexes of the type (η^4-R_4C_4)Fe(μ-CO)$_3$Fe(η^4-C_4R_4) (**3**: R = H[39] and C_6H_5[40]). The structure of the phenyl derivative has been found by X-ray diffraction to be very similar to our tribridged structure of C_{2v}-$Fe_2(CO)_7$ (Figure 6), but with the pair of terminal carbonyl groups on each iron atom replaced by a single tetraphenylcyclobutadiene ligand. The Fe≡Fe distance in (η^4-Ph_4C_4)Fe(μ-CO)$_3$Fe(η^4-C_4Ph_4) (**3**: R = Ph) was found to be 2.18 Å, which is very close to the 2.21 Å Fe≡Fe distance computed for our tribridged C_{2v}-$Fe_2(CO)_7$.

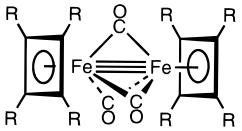

3

Iron carbonyl derivatives containing a formal Fe═Fe bond and two bridging carbonyl groups closely related to the computed energy minimum for $Fe_2(CO)_8$ do not appear to have been isolated and characterized. The closest known compound to $Fe_2(CO)_8$ is the acetylene derivative (μ-$Bu^tC_2Bu^t$)$Fe_2(CO)_6$ (**4**: R = tBu) in which the two bridging carbonyl groups of dibridged C_{2v}-$Fe_2(CO)_8$ are replaced by a bridging alkyne ligand, which is a four-electron donor using electron pairs from each of the orthogonal π-components of the C≡C triple bond.[41] The structure of (μ-$Bu^tC_2Bu^t$)$Fe_2(CO)_6$ is closely related to that of the well-known (μ-RC_2R)$Co_2(CO)_6$ derivatives (**5**) by replacement of the Co−Co single bond in **5** with an Fe═Fe double bond in **4**. Cotton, Jamerson, Stults[41] determined the structures of the exactly analogous (μ-$Bu^tC_2Bu^t$)$M_2(CO)_6$ (M = Co (**5**) and Fe (**4**); R = tBu) derivatives. The metal−metal bond length of 2.46 Å in the dicobalt compound was found to shorten to 2.32 Å in the diiron compound consistent with an increase in the metal−metal bond order from 1 to 2. However, the Fe═Fe bond distance of 2.32 Å in (μ-$Bu^tC_2Bu^t$)$Fe_2(CO)_6$ (**4**: R = tBu) is significantly shorter than the computed Fe═Fe distance of 2.44 Å in the energetically favorable dibridged C_{2v}-$Fe_2(CO)_8$, suggesting a major effect on the Fe═Fe double bond upon changing the bridging groups from carbonyl groups to an alkyne.

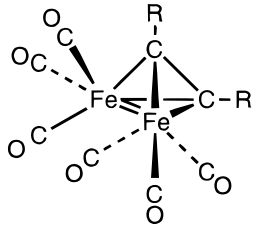

4

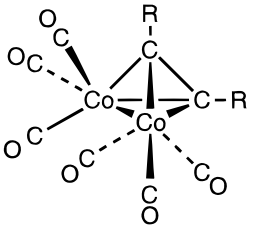

5

Analogues of dibridged C_{2v}-$Fe_2(CO)_8$ retaining the metal−metal double bond and the two bridging carbonyl groups can be obtained if the three terminal carbonyl groups on each iron atom are replaced by a suitable planar hydrocarbon ligand, similar to the conversion of tribridged C_{2v}-$Fe_2(CO)_7$ to the cyclobutadiene derivatives **3** discussed above. The best examples are the dimeric cyclopentadienyl cobalt carbonyl derivatives (η^5-R_5C_5)Co(μ-CO)$_2$Co(η^5-C_5R_5) (**6**: R = H, Me). A structure determination on (η^5-Me_5C_5)Co(μ-CO)$_2$Co(η^5-C_5Me_5) by X-ray crystallography[42] indicates a Co═Co bond distance of 2.33 Å. Returning to an isoelectronic diiron compound by replacing the two bridging carbonyl groups with analogous bridging nitrosyl groups gives (η^5-R_5C_5)Fe(μ-NO)$_2$Fe(η^5-C_5R_5) (**7**: R = H, Me). The Fe═Fe bond length in (η^5-C_5H_5)Fe(μ-NO)$_2$Fe(η^5-C_5H_5) was found by X-ray crystallography[43] also to be 2.33 Å.

(38) Cotton, F. A.; Troup, J. M. *J. Am. Chem. Soc.* **1974**, *96*, 3438.
(39) Fischler, I.; Hildenbrand, K.; Koerner von Gustorf, E. *Angew. Chem., Int. Ed. Engl*. **1975**, *14*, 54.
(40) Murahashi, S.-I.; Mizoguchi, T.; Hosokawa, T.; Montani, I.; Kai, Y.; Kohara, M.; Yasuoka, N.; Kasai, N. *Chem. Commun.* **1974**, 563.
(41) Cotton, F. A.; Jamerson, J. D.; Stults, B. R. *J. Am. Chem. Soc.* **1976**, *98*, 1774.
(42) Orjak, L. M.; Ginsburg, R. E.; Dahl, L. F. *Inorg. Chem.* **1982**, *21*, 940.
(43) Calderón, J. L.; Fontana, S.; Frauendorfer, E.; Day, V. W.; Iske, S. D. A. *J. Organomet. Chem.* **1974**, *64*, C16.

Table 14. Analysis of Vibrational Frequencies (in cm^{-1}) Incorporating Iron−Iron Stretching Character[a]

$Fe_2(CO)_8$	D_{2h}	tetrabridged	267 (62%), 614 (23%), 533 (14%)
	D_{2h}	unbridged	189 (75%), 73 (12%), 185 (9%)
	C_{2h}	distorted unbridged	193 (85%), 93 (5%)
	C_{2v}	dibridged	231 (79%), 619 (5%)
$Fe_2(CO)_7$	C_{2v}	monobridged	274 (73%), 585 (9%)
	C_s	unbridged	238 (81%), 77 (5%), 626 (5%)
	C_{2v}	tribridged	274 (75%), 643 (10%), 521 (9%), 490 (7%)
$Fe_2(CO)_6$	D_{3d}	unbridged	313 (68%), 586 (22%), 455 (8%)
	D_{3h}	unbridged	312 (68%), 585 (20%), 462 (9%)
	D_{2h}	dibridged	275 (75%), 436 (20%), 572 (6%)
	C_{2h}	distorted dibridged	256 (86%), 591 (6%)

[a] The percentages reported reflect the analysis in terms of standard internal coordinates and their B3LYP resulting potential energy distributions (in parentheses, but neglected for those <5%). See Tables 3−13 for complete listings of all vibrational frequencies and infrared intensities.

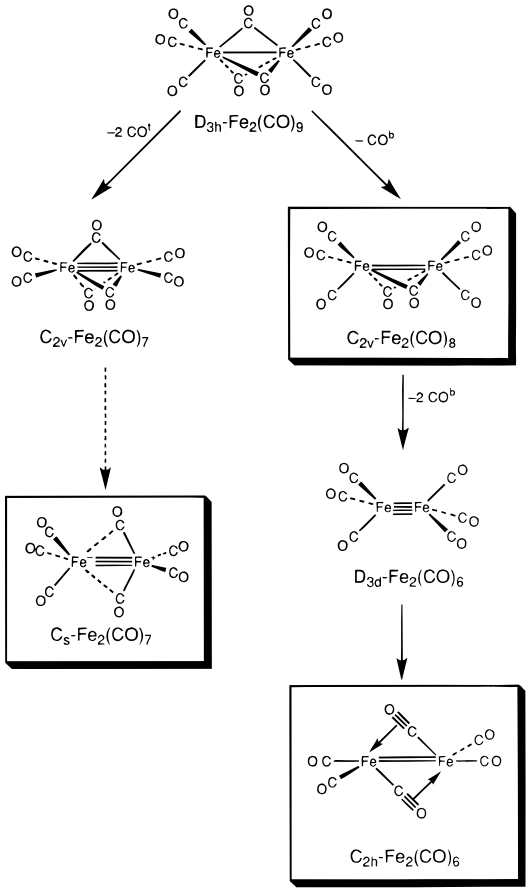

Figure 13. Decarbonylation of the stable $Fe_2(CO)_9$ to give the most stable isomers of $Fe_2(CO)_x$ (x = 8, 7, 6) with the lowest energy structures for a given stoichiometry enclosed in boxes.

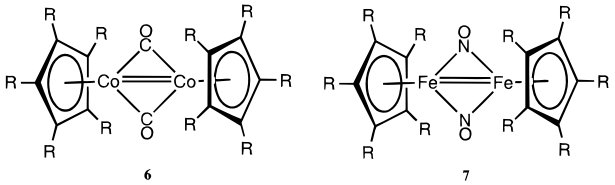

6 **7**

The homoleptic diiron carbonyl with the lowest CO/Fe ratio and highest apparent iron−iron bond order for which a true minimum was found was unbridged D_{3d}-$Fe_2(CO)_6$, which requires an Fe⁴—Fe quadruple bond to give each iron atom the favored 18-electron noble gas configuration. The presence of a metal−metal bond of high bond order is suggested by the very short computed iron−iron bond distance of 2.00 Å, which is in approximate agreement with the 2.09 Å iron−iron distance computed by Reinhold, Hunstock, and Mealli[44] for an unbridged D_{3h}-$Fe_2(CO)_6$ isomer at the SCF level using a simple 3-21G basis set. The σ-bonding network of unbridged $Fe_2(CO)_6$ can consist of two iron sp^3 tetrahedra sharing a vertex similar to the two carbon tetrahedra in ethane, thereby leaving on each metal atom two orthogonal d orbitals, namely the d_{xz} and d_{yz} orbitals, for the two orthogonal π-bonds and two additional d orbitals, namely the d_{xy} and $d_{x^2-y^2}$ orbitals, for a δ bond in the Fe⁴—Fe quadruple bond.

Metal carbonyl derivatives of any type with a metal−metal quadruple bond are unknown and the synthetic prospects for isolating unbridged $Fe_2(CO)_6$ in gram quantities would seem to be very poor for reasons outlined above. However, the principle of replacing the terminal carbonyl groups with a planar hydrocarbon ligand which generates the cyclobutadiene complex **3** from tribridged C_{2v}-$Fe_2(CO)_7$ and the cyclopentadienyl complexes **6** and **7** from dibridged C_{2v}-$Fe_2(CO)_8$ could be applicable to synthesizing a derivative of $Fe_2(CO)_6$ retaining the Fe⁴—Fe quadruple bond, although the product would no longer contain any carbonyl groups. A likely synthetic target might be binuclear arene complexes of the type (η^6-R_6C_6)-Fe⁴—Fe(η^6-C_6R_6) (**8**), which might be synthesized by reaction of iron vapor with the arene, preferably under conditions where iron vapor could be generated with a high concentration of Fe_2 dimers.[35] In this connection, reaction of iron vapor with arenes such as benzene or toluene has long been known to give red-brown unstable matrixes at low temperatures,[45] which revert to iron metal and the arene well below ambient temperature, but which react with a variety of ligands a low temperatures to give the corresponding (arene)FeL_2 complexes (L = PF_3, $P(OR)_3$; 2L = η^4-polyolefins, etc.).[46] Possibly by using a more sterically hindered arene in such an iron vapor experiment, the iron−arene intermediate could be stabilized to the extent that it could be isolated and characterized.

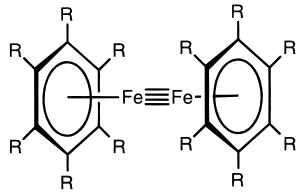

8

Acknowledgment. Dedicated to Professor F. Albert Cotton on the occasion of his 70th birthday. This research was supported by the U. S. National Science Foundation, Grant CHE-9815397. We thank Dr. E. D. Jemmis for the suggestion of the D_{3h} $Fe_2(CO)_6$ structure.

JA001162Y

(44) Reinhold, J.; Hunstock, E.; Mealli, C. *New J. Chem.* **1994**, *18*, 465.

(45) Erner, H. F.; Tevault, D. E.; Fox, W. B.; Smardzewski, R. R. *J. Organomet. Chem.* **1978**, *146*, 45.

(46) Ittel, S. D.; Tolman, C. A. *Organometallics* **1982**, *1*, 1432.